KEK-TH-388A
Fermilab Library
0 1160 0033421 1

KEK-TH-388A
KEK Preprint 93-206
February 1994
H

A Model Independent Analysis of the Electroweak Parameters *

Seiji Matsumoto

Theory Group, KEK, Tsukuba, Ibaraki 305, Japan

and

Department of Physics, Faculty of Science, Kanazawa University, Kanazawa 920, Japan

ABSTRACT

A new framework to study electroweak physics at the one-loop level in general $SU(2)_L \times U(1)_Y$ theories is introduced. It separates the 1-loop corrections into two pieces: process specific ones from vertex and box contributions and the universal ones due to contributions to the gauge boson propagators. The latter are parametrized model-independently in terms of four effective form factors, $\bar{e}^2(q^2)$, $\bar{s}^2(q^2)$, $\bar{g}_Z^2(q^2)$ and $\bar{g}_W^2(q^2)$ correspondingly to $\gamma\gamma$, γZ, ZZ and WW propagators. In addition we introduce one form factor, $\bar{\delta}_b(q^2)$, for the Zb_Lb_L vertex because of its strong dependence on the unknown top quark mass. By assuming only the Standard Model contributions to the process specific corrections except for the Zb_Lb_L vertex, we determine $\bar{g}_Z^2(m_Z^2)$ and $\bar{s}(m_Z^2)$ from the Z parameter measurements, $\bar{g}_Z^2(0)$ and $\bar{s}(0)$ from the low energy neutral current experiments, and $\bar{g}_W^2(0)$ from the W mass measurements. These values are then compared systematically with the predictions of $SU(2)_L \times U(1)_Y$ theories. We also study the quantative significance of the Zb_Lb_L vertex correction $\bar{\delta}_b(m_Z^2)$. The preferred ranges of the top quark and Higgs boson masses within the Standard Model are extracted as functions of $\alpha_s(m_Z)$. The limitations in the theoretical predictions due to the uncertainty in $\bar{\alpha}(m_Z^2)$ are critically discussed. Electroweak physics at TRISTAN is also described in this framework which clarifies the role of each measurement.

FERMILAB
APR 4 1994
LIBRARY

*Talk given at *the 2nd Workshop on TRISTAN Physics at High Luminosities*, Nov. 24-26, 1993, KEK, Ibaraki, Japan. To be published in the proceedings.

National Laboratory for High Energy Physics, 1994

KEK Reports are available from:

Technical Information & Library
National Laboratory for High Energy Physics
1-1 Oho, Tsukuba-shi
Ibaraki-ken, 305
JAPAN

Phone: 0298-64-1171
Telex: 3652-534 (Domestic)
(0)3652-534 (International)
Fax: 0298-64-4604
Cable: KEK OHO
E-mail: LIBRARY@JPNKEKVX (Bitnet Address)
library@kekvax.kek.jp (Internet Address)

1 Introduction

One of the most exciting developments of recent years has been the observation [1] that the electroweak mixing angle $\sin^2\theta_W$ measured precisely at LEP agrees excellently with the prediction of the supersymmetric (SUSY) SU(5) grand unification theory (GUT). The agreement is so impressive that we can hope in the near future to learn about SUSY particle masses [2, 3] with a better measurement of the QCD coupling constant. It has been argued [4] that the uncertainty in the GUT scale particle masses screens any possible effects of SUSY particle threshold corrections to the coupling constant unification condition. The works of refs. [2,3] showed that the non-observation of proton decay effectively constrains the GUT particle contributions to the coupling constant unification and that our hope of learning about the SUSY mass scale from the precision measurements has been revived.

What is exciting about this exercise is that there now seems to be a strong indication that new particles and new interactions may exist at the electroweak scale. They may be produced at the Tevatron, LEP200 and at super colliders. Even prior to their discovery, their effects could be observed in precision experiments through quantum corrections. The effects can be significant if some of the new particles are as light as weak bosons, or if many new particles contribute constructively, or if there exist new strong interactions among them. Even in the absence of such a signal, we can constrain certain new physics possibilities and that we will learn more in the future precision experiments. The purpose of this work is to provide a new framework to confront the electroweak theories with various precision experiments, that allows us to look for new physics beyond the Standard Model in a systematic way at the one-loop level.

In section 2, we briefly review our formalism which can be used for general 4-fermion processes. The S-matrix elements for the neutral and charged currents processes are expressed in terms of the four universal form factors which contain tree-level couplings and radiative effects to the gauge boson propagators, and the process-specific ones which represent the vertex and box corrections. In section 3, we make a systematic analysis according to several steps, using the the data of Z parameter measurements, of the low energy neutral current experiments and of the W mass measurements. Validity of the SU(2)×U(1) gauge theories is checked quantatively, and the q^2-dependence of the two of the four universal form factors is compared with the SM predictions. We also make a detailed analysis for the SM. The dependence of the results on α_s and the uncertainty from the QED effective constant $\alpha(m_Z^2)$ are examined quantitatively. Application of our formalism for the electroweak physics at the TRISTAN energy is

discussed in section 4. We summarize our results in section 5.

2 A new framework for 1-loop electroweak physics

2.1 4 charge form factors

Since what we want to learn from the electroweak precision experiments are the possible effects of new physics beyond the SM, whose exact nature is unknown, we would like to analyse the data in a framework which allows interpretations in wider classes of theoretical models. On the other hand the framework cannot be too general, since our ability to identifying effects of new physics from the precision experiments relies on the renormalizability of the electroweak theory which allows us to predict many observables in terms of a few parameters up to finite quantum corrections. Because the SM corrections are precisely known, those experiments which are sensitive to the quantum effects have a chance to identify a signal of physics beyond the SM. We therefore restrict ourselves to models that respect $SU(2)_L \times U(1)_Y$ gauge symmetry which breaks spontaneously down to $U(1)_{EM}$. In our approach, all new physics contributions that do not respect the spontaneously broken $SU(2)_L \times U(1)_Y$ gauge symmetry can be identified by our inability to fit the data successfully within our framework: these exotic interactions include all non-renormalizable effective interactions among light quarks and leptons that may arise from an exchange of a heavy particle such as a new gauge boson or leptoquark boson, or from new strong interactions that bind common constituents of quarks and leptons.

Our restriction on the electroweak gauge group implies in the tree level that all quarks and leptons couple to the electroweak gauge bosons universally with the same coupling constant as long as they have common electroweak quantum numbers. This universality of the gauge boson coupling to quarks and leptons can in general be violated at the quantum level. It has widely been recognized, however, that this universality of the couplings holds true even in the one-loop level in a wider class of models where new particles affect the precision experiments only via their effects on the electroweak gauge boson propagators [7–14]. This class of effects due to new physics is often called oblique [7, 11] or propagator [13] corrections or those satisfying generalized universality [14]. This concept of universality can be generalized to certain vertex corrections with the non-standard weak boson interactions [15]. It is also sometimes useful in theories with intrinsic vertex and box corrections, such as the SUSY-SM, since the propagator corrections are often larger than the vertex/box ones: propagator corrections can be significant either because of a large multiplicity of contributing particles or

Table 1

	accurately measured parameters	precisely known parameters	parameters to test a theory
γ ~~●~~ γ	$\bar{e}^2(0)$ *	$\alpha = \bar{e}^2(0)/4\pi$	*
γ ~~●~~ Z	$\bar{s}^2(0)$ $\bar{s}^2(m_Z^2)$		$\bar{s}^2(0)$ $\bar{g}_Z^2(m_Z^2)$
Z ~~●~~ Z	m_Z $\bar{g}_Z^2(0)$ $\bar{g}_Z^2(m_Z^2)$	m_Z	$\bar{s}^2(0)$ $\bar{g}_Z^2(m_Z^2)$
W ~~●~~ W	m_W $\bar{g}_W^2(0)$ *	$4\sqrt{2}G_F = \frac{\bar{g}_W^2(0)}{m_W^2}(1+\bar{\delta}_G)$	$\bar{g}_W^2(0)$ *

by a presence of a relatively light new particle, whereas the vertex and box corrections depend on a specific combination of new particles that match the quantum number of the process and are suppressed if one of them is heavy. Our framework adopts this distinction between new physics contributions to the gauge boson propagators and the rest, where we allow the most general contributions in the former whereas we consider only the SM contributions to the latter (vertex and box corrections).

The new physics degree of freedom is then expressed in terms of four charge form factors, each associated with one of the four types of the electroweak gauge boson propagators :

$$\bar{e}^2(q^2) = \hat{e}^2[1 - \mathrm{Re}\,\overline{\Pi}_{T,\gamma}^{\gamma\gamma}(q^2)] \quad \text{for the } \gamma\gamma \text{ propagator,} \tag{1a}$$

$$\bar{s}^2(q^2) = \hat{s}^2[1 + \frac{\hat{c}}{\hat{s}}\mathrm{Re}\,\overline{\Pi}_{T,\gamma}^{\gamma Z}(q^2)] \quad \text{for the } \gamma Z \text{ propagator,} \tag{1b}$$

$$\bar{g}_Z^2(q^2) = \hat{g}_Z^2[1 - \mathrm{Re}\,\overline{\Pi}_{T,Z}^{ZZ}(q^2)] \quad \text{for the } ZZ \text{ propagator,} \tag{1c}$$

$$\bar{g}_W^2(q^2) = \hat{g}^2[1 - \mathrm{Re}\,\overline{\Pi}_{T,W}^{WW}(q^2)] \quad \text{for the } WW \text{ propagator,} \tag{1d}$$

where the hatted couplings $\hat{e} = \hat{g}\hat{s} = \hat{g}_Z\hat{s}\hat{c}$ and the propagator functions are renormalized in the $\overline{\mathrm{MS}}$ scheme. The gauge boson two-point functions that appear in eq.(1) are defined as

$$\overline{\Pi}_{T,V}^{AB}(q^2) = \frac{\overline{\Pi}_T^{AB}(q^2) - \overline{\Pi}_T^{AB}(m_V^2)}{q^2 - m_V^2}, \tag{2}$$

where m_V is the pole mass of the gauge boson V ($m_\gamma = 0$) and the subscript T stands for the transverse part of the vacuum polarization tensor $\Pi_{\mu\nu}(q)$. The propagators are calculated in the 'tHooft-Feynman gauge and the so-called pinch term [8,20,21] of the vertex functions due to diagrams with the weak boson self-couplings are included in the overlined functions $\overline{\Pi}_T^{AB}(q^2)$.

In addition to these four form factors we have the two weak boson masses m_W and m_Z as the parameters of the electroweak theory. Since the charge form factors are

real continuous functions of q^2, we have infinite degrees of free parameters when we use them to parametrize a theory. In practice, however, these charge form factors can be measured accurately enough only at specific q^2 ranges; all four of them at $q^2 = 0$ ($q^2 \ll m_Z^2$), and two of them, $\bar{s}^2(q^2)$ and $\bar{g}_Z^2(q^2)$, at $q^2 = m_Z^2$. Hence, we have just 8 parameters that are measured accurately to test a theory. Among these 8 parameters, three are known precisely; α, G_F and m_Z. Since the gauge boson properties are fixed at

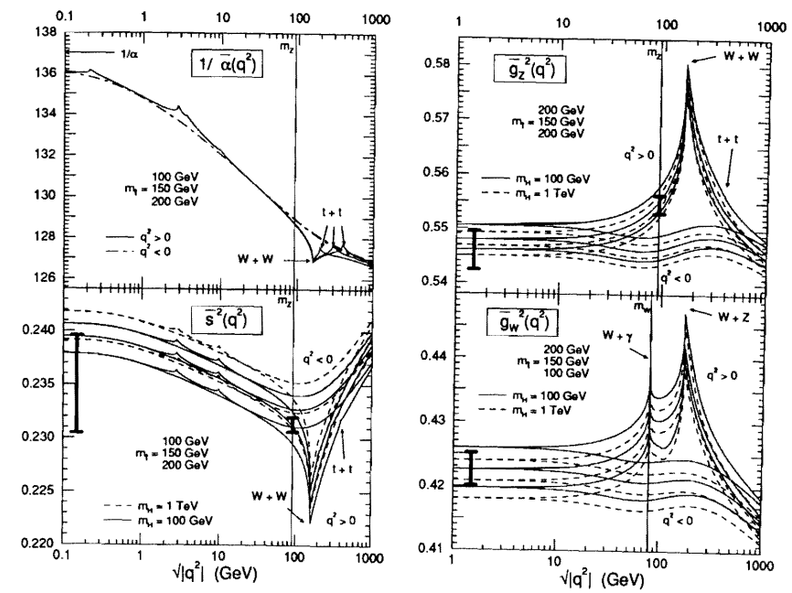

Fig. 1 Four charge form factors in the minimal SM as functions of the momentum tranfer scale. The five thick bars show the 1-σ allowed range of the form factors as obtained by the present analysis of the electroweak precision experiments. The SM predictions are given for m_t =100, 150, 200 GeV and m_H =100, 1000 GeV. Parametrization [19] of the hadronic vacuum polarization contribution is used in the space-like region ($-m_Z^2 < q^2 < 0$). In the time-like region ($q^2 > 0$) only the heavy quark (c, b, t) contributions are taken into acount with the two-loop perturbative QCD correction [42] at $\alpha_s(m_Z) = 0.12$. The light quark contribution at $|q^2| > m_Z^2$ are calculated in perturbative QCD by requiring the continuity at $q^2 = m_Z^2$.

tree level by the three parameters in general models with the SU(2) × U(1) symmetry broken by a vacuum expectation value, we can use the remaining 5 parameters to test the theory at the quantum level: see Table 1. We therefore first determine the 5 parameters, $\bar{s}^2(m_Z^2)$, $\bar{g}_Z^2(m_Z^2)$, $\bar{s}^2(0)$, $\bar{g}_Z^2(0)$, and $\bar{g}_W^2(0)$, from precision experiments, and then confront their values with various theoretical predictions.

When the new physics scale is significantly higher than the scale ($\lesssim m_Z^2$) of precision measurements, we can often neglect new physics contributions to the running of the charge form factors. Among our 5 parameters, the values of $\bar{s}^2(0)$ and $\bar{g}_Z^2(0)$ can then be determined from $\bar{s}^2(m_Z^2)$ and $\bar{g}_Z^2(m_Z^2)$, respectively, by the SM physics only. The effective number of the free parameters is then 3, which corresponds precisely to that of S, T, U [11], ϵ_1, ϵ_2, ϵ_3 [13], or other related triplets of parameters in refs. [12]. When the scale of new physics that couples to gauge boson propagators is near or below the weak boson masses, we may identify its signal as an anomalous running of the charge form factors. This point has been emphasized in refs. [16] in connection with possible existence of the light SUSY particles. The triplet parametrizations are then no longer sufficient to account for new physics degrees of freedom, and we should regard all 5 parameters in the Table 1 as free parameters. Several alternative approaches to the same problem have been proposed in refs. [16–18].

In the minimal SM, all the quantum corrections are determined by just two parameters, m_t and m_H, and hence all the charge form factors are determined by their values. We show in Fig. 1 the four charge form factors in the SM. The trajectories are fixed such that they give correct values for the 3 precisely known parameters, α, G_F, and m_Z (see section 2.4). The 5 parameters that we determine from precision experiments are also shown as 'data' points in the figures, which we will explain in Section 3. It is clear that these 'data' are perfectly consistent with the predictions of the minimal SM, for a certain (m_t, m_H) range, and that no indication of new physics is found. It should be noted here that there is no good measurement of the charge form factors $\bar{e}^2(q^2)$ and $\bar{g}_W^2(q^2)$ except at low energies $q^2 \sim 0$. We may expect TRISTAN and HERA to measure them, and it is challenging to achieve an accuracy comparable to those achieved in the low energy neutral current experiments ($\bar{s}^2(0)$ and $\bar{g}_Z^2(0)$).

2.2 S-matrix elements

All the precision experiments that are sensitive to electroweak physics at the one loop level have so far been confined to those processes with external light quarks and leptons, where their masses can safely be neglected as compared to the weak boson masses in the electroweak one-loop amplitudes. They are the Z boson properties as

measured at LEP and SLC, the neutral current (NC) processes at low energies ($\ll m_Z$), the charged current (CC) processes at low energies and the W mass measurements at the $p\bar{p}$ colliders. The relevant observables in these processes are expressed in terms of the S-matrix elements of four external light fermions which form a scalar product of two chirality conserving currents. All the information on the electroweak physics can be learned by studying the scalar amplitude multiplying these current-current products.

For example, we parameterize the S-matrix element of the NC process $ij \to ij$ (or any one of its crossed channels) as

$$T_{ij} = M_{ij} J_i \cdot J_j, \tag{3}$$

where J_i^μ and J_j^μ denote the bare currents without the coupling factor: $J_i^\mu = \bar{\psi}_f \gamma^\mu P_\alpha \psi_f$ for $i = f_\alpha$, where $P_L = (1-\gamma_5)/2$ and $P_R = (1+\gamma_5)/2$ are the chiral projectors. All the one-loop corrections appear in the scalar amplitudes M_{ij} which depend on flavor and chirality of the currents and on the invariant momentum transfers s and t of the process.

In the neutral current amplitudes, the photonic corrections attached only to the external fermion lines are gauge invariant in themselves. Therefore we can obtain finite and gauge invariant amplitudes by excluding all the external photonic corrections. We find e.g. for the process $i\bar{i} \to j\bar{j}$ the following closed form in the one-loop order

$$\begin{aligned}
M_{ij}^{NC} = {} & \frac{Q_i Q_j}{s}[\bar{e}^2(s) + \hat{e}^2(\Gamma_1^i + \Gamma_1^j)(s) - i\hat{e}^2\Delta_{\gamma\gamma}(s)] + \hat{e}^2[(Q_i I_{3j})\frac{\overline{\Gamma}_2^j(s)}{s} + (I_{3i}Q_j)\frac{\overline{\Gamma}_2^i(s)}{s}] \\
& + \frac{1}{s - m_Z^2 + is\frac{\Gamma_Z}{m_Z}} \\
& \times\{(I_{3i} - Q_i\hat{s}^2)(I_{3j} - Q_j\hat{s}^2)[\bar{g}_Z^2(s) + \hat{g}_Z^2(\Gamma_1^i + \Gamma_1^j)(s) - i\hat{g}_Z^2\Delta_{ZZ}(s)] \\
& \quad + (I_{3i} - Q_i\hat{s}^2)\hat{g}_Z^2[I_{3j}(\hat{c}^2\overline{\Gamma}_2^j + \Gamma_3^j)(s) + \Gamma_4^j(s) - Q_j(\bar{s}^2(s) - \hat{s}^2 + i\Delta_{\gamma Z}(s))] \\
& \quad + (I_{3j} - Q_j\hat{s}^2)\hat{g}_Z^2[I_{3i}(\hat{c}^2\overline{\Gamma}_2^i + \Gamma_3^i)(s) + \Gamma_4^i(s) - Q_i(\bar{s}^2(s) - \hat{s}^2 + i\Delta_{\gamma Z}(s))]\} \\
& + B_{ij}^{NC}(s,t).
\end{aligned} \tag{4}$$

Here the hatted couplings $\hat{e} = \hat{g}\hat{s} = \hat{g}_Z\hat{s}\hat{c}$ are renormalized in the $\overline{\text{MS}}$ scheme, and three of the four charge form factors of eq.(1), $\bar{e}^2(s)$, $\bar{s}^2(s)$ and $\bar{g}_Z^2(s)$ are identified:

$$\bar{e}^2(q^2) = \hat{e}^2[1 - \text{Re}\,\overline{\Pi}_{T,\gamma}^{\gamma}(q^2)], \tag{5a}$$

$$\bar{s}^2(q^2) = \hat{s}^2[1 + \frac{\hat{c}}{\hat{s}}\text{Re}\,\overline{\Pi}_{T,\gamma}^{Z}(q^2)], \tag{5b}$$

$$\bar{g}_Z^2(q^2) = \hat{g}_Z^2[1 - \text{Re}\,\overline{\Pi}_{T,Z}^{ZZ}(q^2)]. \tag{5c}$$

Imaginary parts of the propagator correction factors are denoted by $\Delta_{\gamma\gamma}(s)$, $\Delta_{\gamma Z}(s)$ and $\Delta_{ZZ}(s)$ which are defined as

$$\Delta_{\gamma\gamma}(q^2) = \mathrm{Im}\,\overline{\Pi}^{\gamma\gamma}_{T,\gamma}(q^2), \tag{6a}$$

$$\Delta_{\gamma Z}(q^2) = \hat{s}\hat{c}\,\mathrm{Im}\,\overline{\Pi}^{Z}_{T,\gamma}(q^2), \tag{6b}$$

$$\Delta_{ZZ}(q^2) = \mathrm{Im}\,\overline{\Pi}^{ZZ}_{T,Z}(q^2) - \frac{\mathrm{Im}\,\overline{\Pi}^{ZZ}_{T}(m_Z^2)}{m_Z^2}. \tag{6c}$$

The last equation is a consequence of the LEP convention for m_Z and Γ_Z. The vertex functions $\Gamma^{f_\alpha}_n(s)$ and the box functions $B_{f_\alpha f'_\beta}(s,t)$ are process specific. We first note that the residues of the γ and Z poles are separately physical observables (μ-independent and gauge invariant). At $q^2 = 0$, we find

$$\Gamma^{f_\alpha}_1(0) = \overline{\Gamma}^{f_\alpha}_2(0) = 0 \tag{7}$$

for all f_α, which are ensured by the Abelian and non-Abelian parts of the Ward identities, respectively. The universal residue of the photon pole gives the square of the unit electric charge $\bar{e}^2(0) = 4\pi\alpha$.

The overlines on the vertex functions $\overline{\Gamma}^{f_L}_2(s)$ indicates the removal of the pinch term [8,21]. The vertex functions $\Gamma^{f_\alpha}_3(s)$ are proportional to the square of the fermion mass inside the loop, and are non-negligible only for $f_\alpha = b_L$ in the SM. The functions $\Gamma^{f_\alpha}_4(s)$ are vanishing for all f_α in the SM, though they appear in extended models such as the minimal SUSY-SM. We shall see that the box functions $B_{ij}(s,t)$ are significant only at low energy NC processes and in μ-decay at $s = t = 0$. It is worth noting here that the box contributions to the helicity amplitudes can be expressed in the above simple current product form only when the external fermion masses can be neglected in the loop amplitude. All the vertex and box functions are known precisely in the SM. If we assume no new physics contributions to these process specific (f_α-dependent) corrections, we can determine the three form factors $\bar{e}^2(q^2)$, $\bar{g}^2_Z(q^2)$ and $\bar{s}^2(q^2)$ from the precision experiments independent of further model assumptions.

For the charged current (CC) process $ij \to i'j'$, we find similarly

$$M^{CC}_{ij} = \frac{1}{t - m_W^2}\{\bar{g}^2_W(t) + \hat{g}^2[\Gamma^{ii'}_1 + \Gamma^{jj'}_1 + \overline{\Gamma}^{ii'}_2 + \overline{\Gamma}^{jj'}_2](t)\} + B^{CC}_{ij}(s,t), \tag{8}$$

off the W pole, with an appropriate CKM factor $V_{ii'}V^*_{jj'}$. Precise values of the CC matrix elements are needed only at low energies, and we find for the muon decay constant

$$G_F = \frac{\bar{g}^2_W(0) + \hat{g}^2\bar{\delta}_G}{4\sqrt{2}m_W^2}. \tag{9}$$

Here the factor $\bar{\delta}_G$ denotes the sum of the vertex and the box contributions, whose value is precisely known ($\bar{\delta}_G = 0.0055$) in the SM. Eq.(9) gives the physical W mass in terms of G_F once the $\bar{\delta}_G$ value is known for a given model. The overline here again indicates the removal of the pinch terms and that its numerical value is significantly (about 25%) smaller than the standard factor [25].

2.3 Zb_Lb_L vertex

The only vertex whose magnitude is not yet known in the SM is the Zb_Lb_L vertex which depends strongly on the assumed top quark mass [33]. Hence we find it convenient to introduce one extra form factor

$$\bar{\delta}_b(s) = \Gamma^{b_L}_1(s) + \hat{c}^2\overline{\Gamma}^{b_L}_2(s) + \Gamma^{b_L}_3(s) \tag{10}$$

in our analysis. A similar strategy has been proposed in ref. [17]. An advantage is that the parameter $\bar{\delta}_b$ allows us to determine the quantitative significance of the Zb_Lb_L vertex correction [34], independent of the specific SM mechanism. Furthermore, it

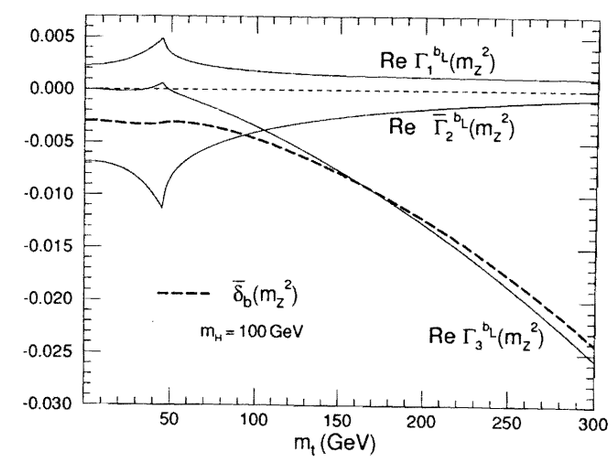

Fig. 2 The m_t-dependence of the Zb_Lb_L vertex form factors $\Gamma^{b_L}_1(m_Z^2)$, $\overline{\Gamma}^{b_L}_2(m_Z^2)$, $\Gamma^{b_L}_3(m_Z^2)$ (solid lines) and $\bar{\delta}_b(m_Z^2)$(long dashed line). $\bar{\delta}_b(m_Z^2)$ is calculted including the known 2-loop effects [35–37] for $m_H = 100\,\mathrm{GeV}$ and $\alpha_s = 0.12$(long dashed line).

allows us to separate the data analysis stage from the evaluation of $\bar{\delta}_b$ in a specific model, that includes $O(\alpha_s m_t^2)$ [35] and $O(m_t^4)$ [36, 37] two-loop corrections of the SM. The m_t-dependence of the vertex form factors $\Gamma_1^{b_L}(m_Z^2)$, $\overline{\Gamma}_2^{b_L}(m_Z^2)$, $\Gamma_3^{b_L}(m_Z^2)$ and $\bar{\delta}_b(m_Z^2)$ in the SM are shown in Fig. 2.

2.4 Constraints due to α, G_F, m_Z

When the basic three parameters of the models with the $SU(2)_L \times U(1)_Y$ symmetry broken by just one vacuum expectation value are renormalized by the three well-known quantities α, G_F and m_Z, all the predictions of the theory are determined at the tree level. It is therefore convenient to introduce three parameters which are proportional to the finite quantum correction effects only. Among the various proposals in the literature [11–13], we find that the S, T, U parameters of Peskin and Takeuchi [11]

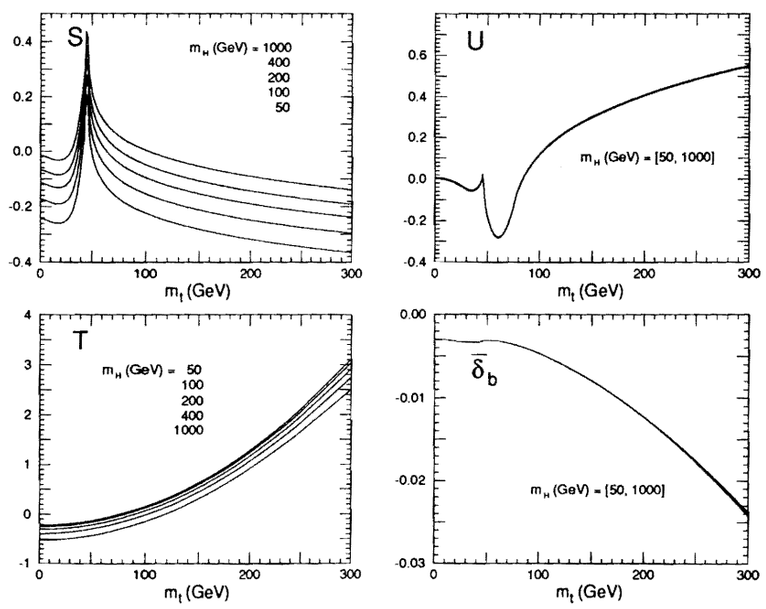

Fig. 3 The SM predictions for the (S, T, U, $\bar{\delta}_b$) parameters as defined in eqs.(11,10) as functions of m_t for selected m_H values. We set $\alpha_s = 0.12$ in the two-loop $O(\alpha_s)$ corrections for S, T, U [42] and $\bar{\delta}_b(m_Z^2)$ [35].

is most convenient if they are extended to include the SM contributions as well. We *define* these parameters in terms of our two-point functions with the pinch terms [21], which are related to our charge form factors as follows:

$$S \equiv 16\,\pi\,\mathrm{Re}\left[\overline{\Pi}^{3Q}_{T,\gamma}(m_Z^2) - \overline{\Pi}^{33}_{T,Z}(0)\right] = \frac{4\bar{s}^2(m_Z^2)\bar{c}^2(m_Z^2)}{\bar{\alpha}(m_Z^2)} - \frac{16\pi}{\bar{g}_Z^2(0)}\,, \tag{11a}$$

$$\alpha T \equiv 4\sqrt{2}\,G_F\,\mathrm{Re}\left[\overline{\Pi}^{33}_{T}(0) - \overline{\Pi}^{11}_{T}(0)\right] = 1 + \bar{\delta}_G - \frac{4\sqrt{2}G_F m_Z^2}{\bar{g}_Z^2(0)}\,, \tag{11b}$$

$$U \equiv 16\,\pi\,\mathrm{Re}\left[\overline{\Pi}^{33}_{T,Z}(0) - \overline{\Pi}^{11}_{T,W}(0)\right] = \frac{4\bar{s}^2(m_Z^2)}{\bar{\alpha}(m_Z^2)} - \frac{16\pi}{\bar{g}_W^2(0)}\,. \tag{11c}$$

These definitions allow us to express all the charge form factors and hence all experimental observables in terms of the three parameters S, T and U without separating the SM contributions to the gauge boson propagators. First, the form factor $\bar{g}_Z^2(0)$ is determined from T via eq.(11b). Second, the form factor $\bar{s}^2(m_Z^2)$ is determined from S via eq.(11a). And finally the form factor $\bar{g}_W^2(0)$ is determined from U via eq.(11c):

$$\frac{1}{\bar{g}_Z^2(0)} = \frac{1 + \bar{\delta}_G - \alpha T}{4\sqrt{2}\,G_F\,m_Z^2} \tag{12a}$$

$$\bar{s}^2(m_Z^2) = \frac{1}{2} - \sqrt{\frac{1}{4} - \bar{e}^2(m_Z^2)\left(\frac{1}{\bar{g}_Z^2(0)} + \frac{S}{16\,\pi}\right)} \tag{12b}$$

$$\frac{1}{\bar{g}_W^2(0)} = \frac{\bar{s}^2(m_Z^2)}{\bar{e}^2(m_Z^2)} - \frac{1}{16\,\pi}(S + U) \tag{12c}$$

The running of these form factors is determined by their defining equations (1) by properly performing the renormalization group improvement:

$$\frac{\bar{s}^2(q^2)}{\bar{e}^2(q^2)} - \frac{\bar{s}^2(m_Z^2)}{\bar{e}^2(m_Z^2)} = \mathrm{Re}\left[\overline{\Pi}^{3Q}_{T,\gamma}(q^2) - \overline{\Pi}^{3Q}_{T,\gamma}(m_Z^2)\right] \tag{13a}$$

$$\begin{aligned}\frac{1}{\bar{g}_Z^2(q^2)} - \frac{1}{\bar{g}_Z^2(0)} &= \mathrm{Re}\left[\overline{\Pi}^{33}_{T,Z}(q^2) - \overline{\Pi}^{33}_{T,Z}(0)\right] - 2\,\hat{s}^2\,\mathrm{Re}\left[\overline{\Pi}^{3Q}_{T,Z}(q^2) - \overline{\Pi}^{3Q}_{T,Z}(0)\right] \\ &\quad + \hat{s}^4\,\mathrm{Re}\left[\overline{\Pi}^{QQ}_{T,Z}(q^2) - \overline{\Pi}^{QQ}_{T,Z}(0)\right]\end{aligned} \tag{13b}$$

$$\frac{1}{\bar{g}_W^2(q^2)} - \frac{1}{\bar{g}_W^2(0)} = \mathrm{Re}\left[\overline{\Pi}^{11}_{T,W}(q^2) - \overline{\Pi}^{11}_{T,W}(0)\right] \tag{13c}$$

All the form factors are thus easily calculable for arbitrary models for fixed (α, G_F and m_Z). In fact, the SM curves in Figs. 1 are obtained this way. By assuming only the SM contribution to the muon decay vertex and box corrections in $\bar{\delta}_G$ and by assuming the SM running of the form factors, especially for $\bar{\alpha}(q^2)$, we can express all the charge form factors as a power series in the above three parameters. To first order, we find

$$\bar{g}_Z^2(0) = 0.5456 \qquad + 0.0040T, \tag{14a}$$

$$\bar{s}^2(m_Z^2) = 0.2334 + 0.0036S - 0.0024T \qquad - 0.0026\delta_\alpha, \tag{14b}$$

$$\bar{g}_W^2(0) = 0.4183 - 0.0031S + 0.0044T + 0.0035U - 0.0015\delta_\alpha, \tag{14c}$$

where we added the shifts due to the uncertainty in the estimated $1/\bar{\alpha}(m_Z^2)$ value, δ_α, which is as large as ± 0.10 [19]. It is clearly seen that $\bar{g}_Z^2(0)$ measures T, $\bar{s}^2(m_Z^2)$ measures a combination of S and T, whereas $\bar{g}_W^2(0)$ measures a combination of all three parameters.

The SM predictions for S, T, U and $\bar{\delta}_b(m_Z^2)$ are shown in Fig.3 as functions of m_t for selected values of m_H, by including all the known two-loop corrections of $O(m_t^4)$ [36,37,41] and of $O(\alpha_s)$ [35,42] at $\alpha_s(m_Z) = 0.12$. From Fig.3, one can see that the parameters S and T show mild sensitivity to m_H, but the parameters U and $\bar{\delta}_b(m_Z^2)$ are almost independent of m_H.

3 Systematic Analysis

In this section, we make a systematic analysis in the following steps, by systematically strengthening the assumptions underlying the analyses:

1. First, by assuming that the precisely known SM contributions dominate the process specific vertex and box corrections, we determine the universal charge form factors from the precision experiments: $\bar{g}_Z^2(m_Z^2)$ and $\bar{s}(m_Z^2)$ from the Z parameter measurements, $\bar{g}_Z^2(0)$ and $\bar{s}(0)$ from the low energy neutral current experiments, and $\bar{g}_W^2(0)$ from the W mass measurements at $p\bar{p}$ colliders. The Zb_LZ_L vertex form factor $\bar{\delta}_b(q^2)$ at $q^2 = m_Z^2$ is fitted simultaneously with the data. New physics contributions that do not respect the spontaneously broken $SU(2)_L \times U(1)_Y$ gauge symmetry can be identified by our inability to fit the data successfully.

2. Once the charge form factors are determined, we can test the running of the two form factors $\bar{g}_Z^2(q^2)$ and $\bar{s}^2(q^2)$ which are determined both at $q^2 = m_Z^2$ and at $q^2 = 0$. When there exist new particles which are not so heavy ($\lesssim m_Z$), we may identify its signal as an anomalous running of the charge form factors.

3. By assuming further that the q^2-dependence of the charge form factors are governed by the SM physics only, we determine the three universal parameters S, T and U, together with $\bar{\delta}_b(m_Z^2)$. They are sensitive to radiative effects of heavy physics. Here again the assumption of the underlying SU(2)×U(1) gauge symmetry is tested by the χ^2-goodness of the fit, and deviation from the SM can be identified from the fitted S, T, U values.

4. At the final stage, we assume the minimal SM contributions to S, T, U and $\bar{\delta}_b(m_Z^2)$, and examine its χ^2 goodness of the fit as functions of the two unknown parameters m_t and m_H.

At each step, we pay attention to the α_s-dependence of our fits, while the uncertainty from the QED effective coupling constant $\alpha(m_Z^2)$ is examined in the last two steps.

3.1 Determination of the charge form factors from precision experiments

3.1.1 Z boson parameters

The most recent results from experiments at LEP and SLC on the Z boson parameters have been reported in refs. [26,27]. The Z line-shape parameters are determined at LEP as [27]

$$\begin{array}{lcl} m_Z(\mathrm{GeV}) & = & 91.187 \pm 0.007 \\ \Gamma_Z(\mathrm{GeV}) & = & 2.489 \pm 0.007 \\ \sigma_h^0(\mathrm{nb}) & = & 41.56 \pm 0.14 \\ R_\ell = \sigma_h^0/\sigma_\ell^0 & = & 20.763 \pm 0.049 \\ A_{\mathrm{FB}}^{0,\ell} & = & 0.0158 \pm 0.0018 \end{array} \qquad \rho_{\mathrm{corr}} = \begin{pmatrix} 1 & -0.157 & 0.017 & 0.012 & 0.075 \\ & 1 & -0.070 & 0.003 & 0.006 \\ & & 1 & 0.137 & 0.003 \\ & & & 1 & 0.008 \\ & & & & 1 \end{pmatrix} \tag{15}$$

The other electroweak data that we used in our fit are as follows [26,27]:

$$P_\tau = -0.139 \pm 0.014, \tag{16a}$$

$$A_{\mathrm{LR}} = 0.10 \pm 0.044 \qquad (\mathrm{SLD}\ [28]), \tag{16b}$$

$$A_{\mathrm{FB}}^{0,b} = 0.099 \pm 0.006, \tag{16c}$$

$$A_{\mathrm{FB}}^{0,c} = 0.075 \pm 0.015, \tag{16d}$$

$$R_b = \sigma_b^0/\sigma_h^0 = 0.2203 \pm 0.0027 \qquad (\mathrm{LEP} + \mathrm{SLD}). \tag{16e}$$

Significant improvements over the last year have been achieved for many of the above measurements.

These parameters are expressed in terms of the scalar amplitudes (4) as follows. Since most of the formulae are common for LEP/SLC measurements and TRISTAN measurements, we show the expressions at arbitrary s. The LEP/SLC results are obtained by setting $s = m_Z^2$.

First, the cross sections for $e^+e^- \to f\bar{f}$ are given by

$$\begin{aligned}\sigma_f &\equiv \sigma(e^+e^- \to f\bar{f}) \\ &= \frac{s}{48\pi}\Bigg\{ \left(\left|M_{LL}^{ef} + M_{LR}^{ef}\right|^2 + \left|M_{RR}^{ef} + M_{RL}^{ef}\right|^2 \right) \frac{C_{fV}}{2} \\ &\quad + \left(\left|M_{LL}^{ef} - M_{LR}^{ef}\right|^2 + \left|M_{RR}^{ef} - M_{RL}^{ef}\right|^2 \right) \frac{C_{fA}}{2} \Bigg\} \left(1 + \frac{3}{4} Q_f \frac{\alpha(s)}{\pi}\right), \end{aligned} \tag{17}$$

where the factor $\left(1 + \frac{3}{4} Q_f \frac{\alpha(s)}{\pi}\right)$ account for the external QED corrections. Since both at LEP/SLC and TRISTAN energies, the SM box contributions are negligibly small, we neglect the $\cos\theta$-dependence of the box correction factors and use their $\cos\theta = 0\,(s = -2t)$ values throughout the analysis. The factors C_{qV}, C_{qA} for quarks contain the external QCD corrections for the vector part [29] and for the axial vector part [30], together with the finite mass corrections of the final state fermions [31]:

$$\begin{aligned} C_{qV} &= 3\left\{ \frac{\beta_q(3-\beta_q^2)}{2} + \frac{\alpha_s}{\pi} + 1.409\left(\frac{\alpha_s}{\pi}\right)^2 - 12.8\left(\frac{\alpha_s}{\pi}\right)^3 \right. \\ &\quad \left. +12\frac{m_q^2(\sqrt{s})}{s}\left(\frac{\alpha_s}{\pi} + 8.7\left(\frac{\alpha_s}{\pi}\right)^2 + 45.3\left(\frac{\alpha_s}{\pi}\right)^3\right)\right\}, \end{aligned} \tag{18a}$$

$$\begin{aligned} C_{qA} &= 3\left\{ \beta_q^3 + \frac{\alpha_s}{\pi} + (1.409 \mp f(m_t))\left(\frac{\alpha_s}{\pi}\right)^2 - 12.8\left(\frac{\alpha_s}{\pi}\right)^3 \right. \\ &\quad \left. -6\frac{m_q^2(\sqrt{s})}{s}\left(\frac{11}{3}\left(\frac{\alpha_s}{\pi}\right) + 14.286\left(\frac{\alpha_s}{\pi}\right)^2\right)\right\}, \end{aligned} \tag{18b}$$

with $\alpha_s \equiv \alpha_s(\sqrt{s})_{\overline{\rm MS}}$ and

$$\beta_q = \sqrt{1 - \frac{4m_q^2(\sqrt{s})}{s}}, \tag{19}$$

where $m_q(\sqrt{s})$ denotes the $\overline{\rm MS}$ running quark mass as evaluated at the unit-of-mass scale $\sqrt{s}$ [31]. The running masses are calculated in the next-to-leading order [31] for the following pole mass choices:

$$m_c = 1.4 \text{ GeV}, \tag{20a}$$

$$m_b = 4.8 \text{ GeV}. \tag{20b}$$

The $O(\alpha_s^2)$ axial parts contain m_t dependence through the function $f(m_t)$ [30]:

$$f(m_t) = 2\ln\frac{m_Z}{m_t} - \frac{37}{12} + \frac{28}{81}\left(\frac{m_Z}{2\,m_t}\right)^2 + 0.2107\left(\frac{m_Z}{2\,m_t}\right)^4. \tag{21}$$

The minus sign should be taken in front of $f(m_t)$ in eq.(18b) for u, c quarks, and the plus sign for d, s, b quarks. For charged leptons, these factors are given as

$$C_{\ell V} = \frac{\beta_\ell(3-\beta_\ell^2)}{2}, \tag{22a}$$

$$C_{\ell A} = \beta_\ell^3. \tag{22b}$$

with

$$\beta_\ell = \sqrt{1 - \frac{4m_\ell^2}{s}}. \tag{23}$$

When we can neglect the masses of the final leptons (for $\ell = e$ and μ), eq.(17) reduces to a simple one:

$$\sigma_\ell = \frac{s}{48\pi}\left\{\left|M_{LL}^{e\ell}\right|^2 + \left|M_{LR}^{e\ell}\right|^2 + \left|M_{RL}^{e\ell}\right|^2 + \left|M_{RR}^{e\ell}\right|^2\right\}\left(1 + \frac{3}{4}\frac{\alpha(s)}{\pi}\right). \tag{24}$$

On the Z pole, the partial widths Γ_f's, the width ratios R_ℓ and R_b are defined from the cross sections (17) and (24) as

$$\sigma_f = \frac{12\pi}{m_Z^2}\frac{\Gamma_\ell \cdot \Gamma_f}{\Gamma_Z^2}, \tag{25a}$$

$$R_\ell = \sigma_h / \sigma_\ell, \tag{25b}$$

$$R_b = \sigma_b / \sigma_h. \tag{25c}$$

Next, the Forward-Backward asymmetry is given by

$$A_{FB}^{0,\ell} = \frac{3}{4}\frac{\left|M_{LL}^{e\ell}\right|^2 + \left|M_{RR}^{e\ell}\right|^2 - \left|M_{LR}^{e\ell}\right|^2 - \left|M_{RL}^{e\ell}\right|^2}{\left|M_{LL}^{e\ell}\right|^2 + \left|M_{RR}^{e\ell}\right|^2 + \left|M_{LR}^{e\ell}\right|^2 + \left|M_{RL}^{e\ell}\right|^2}, \tag{26}$$

for leptons, and

$$A_{\rm FB}^{0,q} = \frac{3}{4}\frac{2\beta_q\left\{\left|M_{LL}^{eq}\right|^2 + \left|M_{RR}^{eq}\right|^2 - \left|M_{LR}^{eq}\right|^2 - \left|M_{RL}^{eq}\right|^2\right\}}{\frac{3-\beta_q^2}{2}\left\{\left|M_{LL}^{eq} + M_{LR}^{eq}\right|^2 + \left|M_{RL}^{eq} + M_{RR}^{eq}\right|^2\right\} + \beta_q^2\left\{\left|M_{LL}^{eq} - M_{LR}^{eq}\right|^2 + \left|M_{RL}^{eq} - M_{RR}^{eq}\right|^2\right\}}, \tag{27}$$

$$\beta_q = \sqrt{1 - \frac{4m_q^2}{m_Z^2}}, \qquad (q = b, c)$$

for quarks ($q = b, c$). The QCD corrections for the FB asymmetries [32] have not been included in eq.(27). The reported asymmetries from LEP $A_{\rm FB}^{0,b}$(LEP) and $A_{\rm FB}^{0,c}$(LEP) have been corrected for theses effects by assuming a linear α_s-dependence and $\alpha_s = 0.12$. We therefore calculate the LEP asymmetries by the following formula;

$$A_{\rm FB}^{0,q}({\rm LEP}) = A_{\rm FB}^{q,0}\frac{1 + k_A\left(\frac{\alpha_s}{\pi}\right)}{1 + k_A\frac{0.12}{\pi}} \tag{28}$$

with $k_A = 0.75$ [27]. The QCD correction depends on details of the final charm and bottom quark tagging procedure, and each experiment should give the α_s-dependence of the corrected asymmetry value.

Table 2 vertex form factors in the SM at $\sqrt{s} = 91.187\,\mathrm{GeV}$

f	Γ_1^f	$\overline{\Gamma}_2^f$	Γ_3^f
ν_L	$0.00252 + 0.00431\,i$	$-0.00680 - 0.00565\,i$	—
ℓ_L	$0.00185 + 0.00325\,i$	$-0.00680 - 0.00565\,i$	—
ℓ_R	$0.00020 + 0.00032\,i$	—	—
u_L	$0.00203 + 0.00354\,i$	$-0.00680 - 0.00565\,i$	—
u_R	$0.00009 + 0.00014\,i$	—	—
d_L	$0.00225 + 0.00389\,i$	$-0.00680 - 0.00565\,i$	—
d_R	$0.00002 + 0.00004\,i$	—	—
$b_L\,(m_t = 100)$	$0.00176 + 0.00107\,i$	$-0.00402 + 0.00000\,i$	$-0.00347 + 0.00000\,i$
$b_L\,(m_t = 150)$	$0.00141 + 0.00107\,i$	$-0.00261 + 0.00000\,i$	$-0.00763 + 0.00000\,i$
$b_L\,(m_t = 200)$	$0.00126 + 0.00107\,i$	$-0.00179 + 0.00000\,i$	$-0.01270 + 0.00000\,i$

Finally, the τ polarization asymmetry and the Left-Right asymmetry are expressed as

$$P_\tau = \frac{\left|M_{LR}^{e\ell}\right|^2 + \left|M_{RR}^{e\ell}\right|^2 - \left|M_{LL}^{e\ell}\right|^2 - \left|M_{RL}^{e\ell}\right|^2}{\left|M_{LR}^{e\ell}\right|^2 + \left|M_{RR}^{e\ell}\right|^2 + \left|M_{LL}^{e\ell}\right|^2 + \left|M_{RL}^{e\ell}\right|^2}, \tag{29}$$

$$A_{\mathrm{LR}} = \frac{\sum_f \left(\left|M_{LL}^{ef}\right|^2 + \left|M_{LR}^{ef}\right|^2 - \left|M_{RL}^{ef}\right|^2 - \left|M_{RR}^{ef}\right|^2\right)}{\sum_f \left(\left|M_{LL}^{ef}\right|^2 + \left|M_{LR}^{ef}\right|^2 - \left|M_{RL}^{ef}\right|^2 - \left|M_{RR}^{ef}\right|^2\right)}. \tag{30}$$

On the Z-pole, these asymmetries ($A_{\mathrm{FB}}^{0,f}, P_\tau, A_{\mathrm{LR}}$) determine $\bar{s}^2(m_Z^2)$ almost independently of $\bar{g}_Z^2(m_Z^2)$, $\bar{\delta}_b(m_Z^2)$ and α_s.

In the absence of an accurate quantitative measurement of the QCD coupling constant and for the convenience of the GUT studies, we choose $\alpha_s \equiv \alpha_s(m_Z)_{\overline{\mathrm{MS}}}$ as an input parameter of our fit, and present the results as functions of α_s.

One can then either add independent data from direct α_s measurements, or study quantitative consequences of a particular GUT model that predicts α_s.

In order to determine the universal charge form factors $\bar{s}^2(m_Z^2)$, $\bar{g}_Z^2(m_Z^2)$ and the Zb_Lb_L vertex form factor $\bar{\delta}_b(m_Z^2)$ through these formulae from the data (15) and (16), we should further estimate the process specific contributions to the vertex and box diagrams. The SM contributions at $\sqrt{s} = m_Z$ to the vertex factors in eq.(4) are given in Table 2, where the corresponding values for the Zb_Lb_L vertex are also listed together for comparison (see Fig. 2). It should be noted that, on the Z-pole, the box contributions are negligible ($\sim O(\alpha_W^2)$) in the cross section as compared to the $O(\alpha_W)$ propagator and vertex corrections.

We now assume the SM dominance to the vertex and box corrections except for the Zb_Lb_L vertex, and make a fit in terms of the three parameters $\bar{s}^2(m_Z^2)$, $\bar{g}_Z^2(m_Z^2)$ and $\bar{\delta}_b(m_Z^2)$. The overall fit to all the Z parameters listed above gives

$$\begin{aligned} \bar{g}_Z^2(m_Z^2) &= 0.5546 - 0.031\,(\alpha_s - 0.12) \pm 0.0017 \\ \bar{s}^2(m_Z^2) &= 0.2313 + 0.008\,(\alpha_s - 0.12) \pm 0.0007 \\ \bar{\delta}_b(m_Z^2) &= -0.0062 - 0.428\,(\alpha_s - 0.12) \pm 0.0035 \end{aligned} \qquad \rho_{\mathrm{corr}} = \begin{pmatrix} 1 & 0.14 & -0.36 \\ & 1 & 0.20 \\ & & 1 \end{pmatrix}, \tag{31a}$$

$$\chi^2_{\min} = 1.66 + \left(\frac{\alpha_s - 0.103}{0.0127}\right)^2, \tag{31b}$$

for a given value of $\alpha_s \equiv \alpha_s(m_Z)_{\overline{\mathrm{MS}}}$; the errors and the correlations are almost independent of α_s.

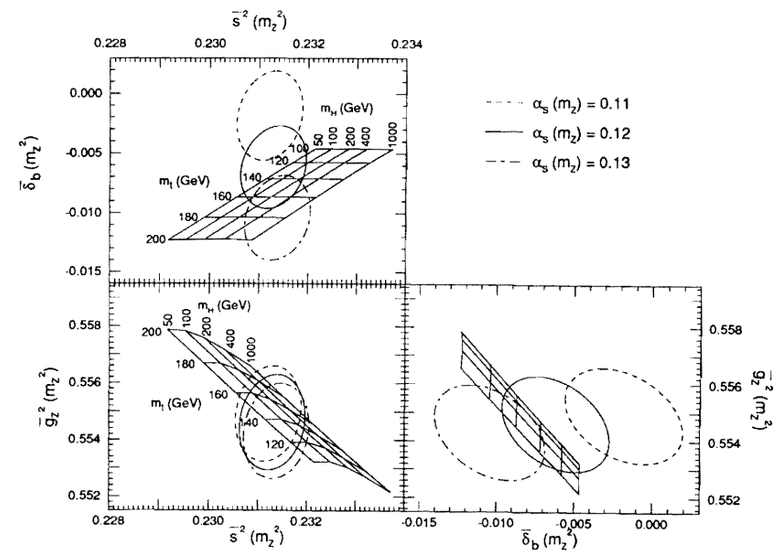

Fig. 4 Three parameter fit to the Z boson parameters for three $\alpha_s(m_Z)$ values. The Zb_Lb_L vertex form factor $\bar{\delta}_b(m_Z^2)$ is introduced as the third parameter of the fit in addition to the two universal charge form factors $\bar{s}^2(m_Z^2)$ and $\bar{g}_Z^2(m_Z^2)$. Also shown are and the SM predictions in the range 100 GeV$< m_t <$200 GeV and 50 GeV$< m_H <$1000 GeV, which are calculated by assuming $(\Delta\frac{1}{\alpha})_{\mathrm{hadrons}} = -3.88$ ($\delta_\alpha = 0$) [19] for the hadronic vacuum polarization contribution to $\bar{\alpha}(m_Z^2)$.

The above results are shown in Fig.4, along with the SM predictions with all known corrections of the $O(m_t^4)$ level [36, 37, 39–41] and of the $O(\alpha_s)$ two-loop corrections [35, 42] in perturbative QCD, but without non-perturbative $t\bar{t}$ threshold effects [43]. The SM prediction to $\bar{s}^2(m_Z^2)$ is also sensitive to the hadronic vacuum polarization correction, for which we take [19] $(\Delta\frac{1}{\alpha})_{\text{hadrons}} = -0.0283/\alpha = -3.88$. Its error $\delta_\alpha = \pm 0.0007/\alpha = \pm 0.10$ leads to a shift in the SM predictions for $\bar{s}^2(m_Z^2)$ by ± 0.00026. The SM predictions in Fig. 4 are obtained by setting $\delta_\alpha = 0$.

We show in Fig. 4 1-σ contours of the fit for three representative α_s values. It is clearly seen that the γZ-mixing parameter $\bar{s}^2(m_Z^2)$ is measured rather independent of α_s, while the Z coupling strength $\bar{g}_Z^2(m_Z^2)$ is negatively correlated with the assumed α_s value, reflecting its sensitivity to the total Z width. This anti-correlation leads to a preference of larger m_t in the SM for smaller α_s. The parameter $\bar{s}^2(m_Z^2)$ is relatively insensitive to α_s because it is measured mainly from the asymmetry parameters that are either completely or almost insensitive to the QCD corrections.

Before leaving the Z parameters, we would like to give two comments on the measurements of the Zb_Lb_L vertex form factor $\bar{\delta}_b(m_Z^2)$ and α_s, which are strongly correlated. As is clearly seen from Fig. 4, the fit to the parameter $\bar{\delta}_b$ depends strongly on α_s, reflecting its sensitivity to R_t and Γ_Z, more than to R_b that measures $\bar{\delta}_b(m_Z^2)$ directly and is rather insensitive to α_s. Because of this sensitivity to α_s, it is not meaningful to quote a bound on $\bar{\delta}_b$, or on m_t from the SM Zb_Lb_L vertex correction, without studying carefully its α_s dependence. It is worth emphasizing here that there is no evidence of the Zb_Lb_L vertex for $\alpha_s \gtrsim 0.13$, as the corresponding parameter for d_L or s_L is about -0.003. For $\alpha_s \lesssim 0.12$, we can obtain rather stringent upper bound on m_t [17, 34] that one can read off from Fig. 4, mainly because there is no good evidence for the large Zb_Lb_L vertex effect. This point has also been emphasized by the LEP electroweak working group [27]. Furthermore, this strong correlation makes the fitted α_s value depend strongly on the assumed $\bar{\delta}_b$ value. If we allow $\bar{\delta}_b$ and α_s to be fitted freely by the data, then the result (31) gives $\bar{\delta}_b(m_Z^2) = 0.0015 \pm 0.0071$ and $\alpha_s(m_Z^2) = 0.103 \pm 0.013$, with $\rho_{\text{corr}} = -0.85$. It is therefore necessary to assume the SM contributions to $\bar{\delta}_b(m_Z^2)$, and to a lesser extent those to $\bar{g}_Z^2(m_Z^2)$, in order to measure α_s from the electroweak Z-parameters. The result of such an analysis is given in section 4.3 where we study consequences of the minimal SM.

3.1.2 Low Energy Neutral Current

We consider in our analysis four types of low energy neutral current experiments. They are the neutrino-nuclei scattering (ν_μ–q), the neutrino-electron scattering (ν_μ–e),

atomic parity violation (APV), and the polarized electron-deuteron scattering experiments (eD). All of them measure the universal form factors $\bar{s}^2(0)$ and $\bar{g}_Z^2(0)$. Effects due to small but finite momentum transfer in these processes are corrected for by assuming that the running of these form factors are determined by the SM particles only (see Fig. 1), which is an excellent approximation at low energies. Vertex and box corrections are performed by assuming that they are dominated by the SM contributions. For each sector, we first give a model-independent parametrization of the data, and then give our fit in the $(\bar{s}^2(0), \bar{g}_Z^2(0))$ plane.

<u>$\nu - q$ **scattering**</u>

For the ν_μ–q data, we used the results of the analysis of ref. [44]. The fitted parameters (g_L^2, g_R^2, δ_L^2, δ_R^2) are, however, dependent on the assumed value of the charmed quark mass (m_c) in the slow-rescaling formula for the charged current cross sections. By using the constraint on m_c from the charged current experiments, $m_c = 1.54 \pm 0.33$ GeV [44], we can properly take into account the m_c dependence of the fit. We thus find a new model-independent parametrization of the ν_μ–q data [6]:

$$\begin{array}{rcl} g_L^2 &=& 0.2980 \pm 0.0044 \\ g_R^2 &=& 0.0307 \pm 0.0047 \\ \delta_L^2 &=& -0.0589 \pm 0.0237 \\ \delta_R^2 &=& 0.0206 \pm 0.0160 \end{array} \qquad \rho_{\text{corr}} = \begin{pmatrix} 1 & -0.559 & -0.163 & 0.162 \\ & 1 & 0.156 & -0.037 \\ & & 1 & -0.447 \\ & & & 1 \end{pmatrix}. \tag{32}$$

The standard model fit is then performed by expressing the above parameters in terms of the ratio of the squares of the NC and CC S-matrix elements of eqs.(4) and (8) evaluated at $\langle -t \rangle_{NC} = \langle -t \rangle_{CC} = 20$ GeV^2. We reproduced the well-known results of ref. [45]. The corrections due to the running of $\bar{s}^2(t)$, the neutrino 'charge radius' factor [46] $\overline{\Gamma}_2^{\nu_\mu}(t)$ of eq.(4), and the WW box are found to be significant. After further correcting for the QED radiation effects in the CC cross section [47], we find

$$\left.\begin{array}{rcl} \bar{g}_Z^2(0) &=& 0.5483 \pm 0.0081 \\ \bar{s}^2(0) &=& 0.2392 \pm 0.0143 \end{array}\right\} \qquad \rho_{\text{corr}} = 0.92, \tag{33a}$$

$$\chi^2_{\text{min}} = 0.86. \tag{33b}$$

The strong positive correlation is a consequence of the smallness of the error of $g_L^2 + g_R^2$ in (32) that measures the total neutral current cross section off isoscalar targets. The above fit is given in Fig. 3 as a 1-σ counter.

<u>$\nu - e$ **scattering**</u>

For the ν_μ–e data, we used the results of CHARM, BNL E374 and CHARM-II [48], which are summarized by R. Beyer [48] as

$$\left.\begin{array}{rcl} (\rho)_{\text{eff}}^{\nu_\mu e} &=& 1.007 \pm 0.028 \\ (\sin^2\theta_W)_{\text{eff}}^{\nu_\mu e} &=& 0.233 \pm 0.008 \end{array}\right\} \qquad \rho_{\text{corr}} = 0.09. \tag{34}$$

The quoted quality of the fit is $\chi^2_{\rm min} = 7.7$ for $d.o.f. = 14$. These effective parameters are obtained from the data by assuming the tree-level formula for the $\nu_\mu e$ and $\bar{\nu}_\mu e$ scattering cross sections.

We can hence obtain the electroweak parameters by evaluating the full matrix elements at an average momentum transfer of these experiments, $\langle -t \rangle \sim m_\mu^2$, and then by expressing the above effective parameters in terms of the radiatively corrected cross sections. We reproduce the known results of ref. [49], and find that the only significant correction comes from the neutrino 'charge radius' factor and the WW box contributions. We find

$$\left.\begin{array}{rcl} \bar{g}_Z^2(0) & = & 0.5459 \pm 0.0153 \\ \bar{s}^2(0) & = & 0.2416 \pm 0.0080 \end{array}\right\} \qquad \rho_{\rm corr} = 0.09 \tag{35}$$

with $\chi^2_{\rm min} = 0$, since we take the fit (34) as the model independent parametrization of the $\nu_\mu - e$ data [48]. The result is also shown in Fig. 3.

Atomic Parity Violation

As for the APV experiments, we used the result of the analysis [50] on the parity violating transitions in the cesium atom (A,Z)=(135,55);

$$Q_W(135,55) = -71.04 \pm 1.81 \tag{36}$$

where we sum the experimental and theoretical errors by quadrature.

Our simple formula (4) reproduces the u- and d-quark contributions of ref. [51], but not the photonic correction to the axial vector Zee vertex nor the $Z\gamma$ box corrections that are sensitive to the nucleon structure. We adopt the results of ref. [51] for these corrections, and find

$$\bar{s}^2(0) = -0.6130 \cdot \bar{g}_Z^2(0) + 0.5661 \pm 0.0083. \tag{37}$$

The result is shown in Fig. 3.

e–D scattering

Finally, for the SLAC eD polarization asymmetry experiment [52], we make a model-independent fit to the original data by using the two parameters, $2C_{1u} - C_{1d}$ and $2C_{2u} - C_{2d}$ of ref. [53], by taking into account uncertainties due to the sea-quark contributions and finite $R = \sigma_L/\sigma_T$ [54], and those due to higher twist contributions [55, 56]. The former uncertainties are found to be very small, confirming the results of ref. [54], while the latter are found to be model dependent [57]. We adopt the estimates [56] based on the MIT-Bag model, which find rather small corrections, as in the neutrino scattering off isoscalar targets [58]. Further study on the higher twist effects may be needed to achieve precision measurements of the electroweak parameters

in these reactions. After allowing for uncertainties in the Bag model parameters of ref. [56], we find

$$\left.\begin{array}{rcl} 2\,C_{1u} - C_{1d} & = & -0.94 \pm 0.26 \\ 2\,C_{2u} - C_{2d} & = & 0.66 \pm 1.23 \end{array}\right\} \qquad \rho_{\rm corr} = -0.975 \tag{38}$$

with $\chi^2_{\rm min} = 9.95$ for 11 data points. Because of the strong correlation, only a linear combination of the two coupling factors is measured well.

The electroweak corrections in the SM are found in ref. [59]. Our formula (4) leads to all relevant correction factors except for the external photonic corrections. We use the explicit form of ref. [51] for these external photonic correction factors, and checked the insensitivity of our fit to the uncertainty in the $Z\gamma$ box corrections. The

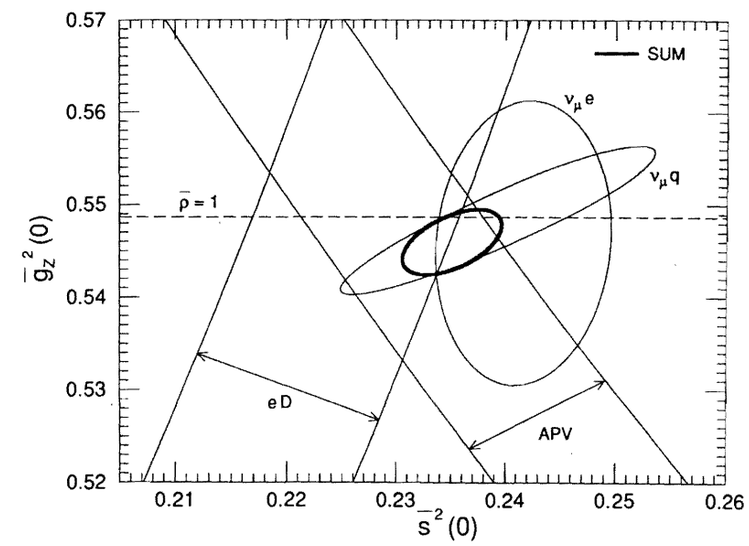

Fig. 5 Fit to the electroweak low energy neutral current data in terms of the two universal charge form factors $\bar{s}^2(0)$ and $\bar{g}_Z^2(0)$. 1-σ contors are shown separately for the ν_μ-q data [44], the ν_μ-e data [48], the atomic parity violation (APV) data [50], and the SLAC e-D polarization asymmetry data [52]. The 1-σ allowed region of the combined fit is shown by thick contor. The straight dashed line shows the 'tree' level prediction of the minimal SM: $\bar{\rho} \equiv \bar{g}_Z^2(0)/(4\sqrt{2}G_F m_Z^2) = 1$.

QED coupling $\bar{e}^2(t)$ and the vertex functions $\Gamma_1(t)$ and $\overline{\Gamma}_2(t)$ in our amplitudes (4) are evaluated at $\langle -t \rangle = 1.5\text{GeV}^2$. We find

$$\bar{s}^2(0) = 0.3264 \cdot \bar{g}_Z^2(0) + 0.0471 \pm 0.0094, \tag{39a}$$

$$\chi^2_{\min} = -1.78 \cdot \bar{g}_Z^2(0) + 1.44, \tag{39b}$$

where again we take the fit (38) as the model-independent parametrization of the data. The above parametrization is valid only in the vicinity of the SM predictions, $\bar{g}_Z^2(0) \sim 0.55$, as shown in Fig. 5.

The results of our two parameter fit to all the neutral current data are summarized in Fig. 5 by 1-σ allowed regions in the $(\bar{s}^2(0),\ \bar{g}_Z^2(0))$ plane. They are consistent with each other and, after combining the above four sectors, we find

$$\left.\begin{aligned} \bar{g}_Z^2(0) &= 0.5460 \pm 0.0035 \\ \bar{s}^2(0) &= 0.2351 \pm 0.0045 \end{aligned}\right\} \quad \rho_{\text{corr}} = 0.53, \tag{40a}$$

$$\chi^2_{\min} = 2.89. \tag{40b}$$

The fit is excellent as the effective degrees of freedom of the fit is $8 - 2 = 6$. The combined fit above (40a) is shown by the thick 1-σ contour in Fig. 5.

3.1.3 Charged Current

The W mass data have been updated this summer by the CDF and D0 collaborations [60]. We obtain

$$m_W = 80.25 \pm 0.24\text{GeV} \tag{41}$$

by combining the two most recent measurements [60] after adding all the quoted errors by quadrature.

The electroweak parameter $\bar{g}_W^2(0)$ is then obtained from the μ life-time via the identity (9). By using the SM estimate $\bar{\delta}_G = 0.0055$ and the perturbative approximation $\bar{g}^2 = \bar{g}_W^2(0)$, we find

$$\bar{g}_W^2(0) = 0.4226 \pm 0.0025. \tag{42}$$

No other experiment in the charged current sector is accurate enough to add useful information in our electroweak analysis. Precision measurements of the W width [61] and its leptonic branching fraction may determine $\bar{g}_W^2(m_W^2)$ in the future.

All the electroweak precision data have now been represented by the charge form factor values of eqs.(31,40,42). We find that all results are consistent with the assumptions of the $SU(2)_L \times U(1)_Y$ universality and the SM dominance of the vertex and box corrections. In the following, we perform the fit to the data in three steps by systematically strengthening the model assumptions.

3.2 Testing the running of the charge form factors

Only two of the four form factors, $\bar{s}^2(q^2)$ and $\bar{g}_Z^2(q^2)$, have been measured sufficiently accurately at two energy scales, $q^2 = 0$ and m_Z^2. From eqs.(31,40), we find

$$\left.\begin{aligned} \frac{4\pi}{\bar{g}_Z^2(m_Z^2)} - \frac{4\pi}{\bar{g}_Z^2(0)} &= -0.36 + 1.2(\alpha_s - 0.12) \pm 0.16 \\ \frac{\bar{s}^2(m_Z^2)}{\bar{\alpha}(m_Z^2)_{\text{SM}}} - \frac{\bar{s}^2(0)}{\alpha} &= -2.45 + 1.1(\alpha_s - 0.12) \pm 0.63 \end{aligned}\right\}, \quad \rho_{\text{corr}} = -0.48. \tag{43}$$

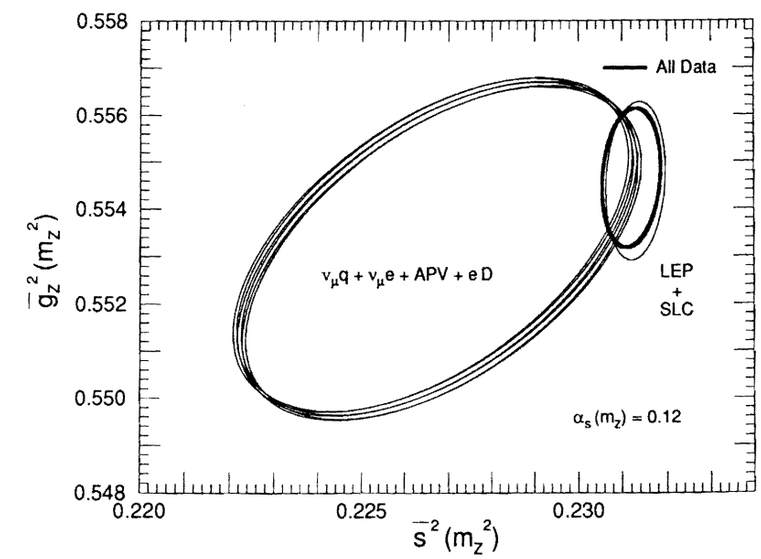

Fig. 6 Two parameter fit to the combined low energy neutral current data and the Z parameters. The latter fit ('LEP+SLC') is copied from Fig. 4 for $\alpha_s(m_Z) = 0.12$. The low energy combined fit of Fig. 5 has been rescaled to the m_Z scale by assuming the SM running of the two charge form factors, $\bar{s}^2(q^2)$ and $\bar{g}_Z^2(q^2)$, which depend on m_t and m_H. The degree of uncertainties in the SM predictions for the running of the form factors is shown by drawing the results for m_t =100, 150, 200 GeV and m_H=100, 100 GeV in the same figure. The 1-σ allowed region of the combined fit is given by the thick contor, for which the above uncertainties give negligible effects.

The SM predictions for these quantities are, respectively

$$\frac{4\pi}{\bar{g}_Z^2(m_Z^2)} - \frac{4\pi}{\bar{g}_Z^2(0)} = -0.2998 + 0.0013\left(\frac{150}{m_t}\right)^2 + 0.0021\left(\frac{100}{m_H}\right)^2, \tag{44a}$$

$$\frac{\bar{s}^2(m_Z^2)}{\bar{\alpha}(m_Z^2)_{\rm SM}} - \frac{\bar{s}^2(0)}{\alpha} = -3.0760 + 0.0058\left(\frac{150}{m_t}\right)^2, \tag{44b}$$

in the range $100 < m_t(\,\mathrm{GeV}) < 250$ and $100 < m_H(\,\mathrm{GeV}) < 1000$. Both results are consistent at the 1-σ level with the assumption that the running of these form factors is governed by the SM particles only (see Fig.6). Since the running of the form factors is affected only by particles of mass in the vicinity of m_Z, we conclude that there is no indication of new particles of mass $\lesssim m_Z$.

The errors in (43) are determined by those of the low energy experiments. Further improvements in the low energy precision experiments are needed to detect a signal of relatively light new particles.

3.3 Testing the 3 parameter universality

By using the SM running of the form factors (44), we can combine the Z parameter fit (31) and the low energy NC fit (40). This is schematically shown in Fig. 6, where the combined low energy NC fit of Fig. 5 is reproduced in the $(\bar{s}^2(m_Z^2),\ \bar{g}_Z^2(m_Z^2))$ plane. The uncertainty in the running of the parameters within the SM is visualized by the thickness of the contour which spans the range $m_t = 100 - 200$ GeV, $m_H = 100 - 1000$ GeV in eq.(44). The low energy parameters are consistent with the Z parameters, which are also shown as the 'LEP+SLC' contour. All the neutral current data are now combined to give

$$\begin{aligned} \bar{g}_Z^2(m_Z^2) &= 0.5547 - 0.023(\alpha_s - 0.12) \pm 0.0015 \\ \bar{s}^2(m_Z^2) &= 0.2312 + 0.008(\alpha_s - 0.12) \pm 0.0007 \\ \bar{\delta}_b(m_Z^2) &= -0.0064 - 0.435(\alpha_s - 0.12) \pm 0.0034 \end{aligned} \qquad \rho_{\rm corr} = \begin{pmatrix} 1 & 0.16 & -0.31 \\ & 1 & 0.20 \\ & & 1 \end{pmatrix}, \tag{45a}$$

$$\chi^2_{\rm min} = 5.50 + ((\alpha_s - 0.103)/0.0125)^2. \tag{45b}$$

The above fit is almost independent of $(m_t,\ m_H)$ values assumed in the running of the charge form factors. The $\chi^2_{\rm min}$ value of 7.3 for $\alpha_s = 0.12$ is excellent for the effective degrees of freedom of the fit, $18 - 3 = 15$.

There is one notable point at this stage which becomes apparent by comparing the global fit of Fig. 6 with the individual fit to low energy NC data in Fig. 5. Both the data on ν_μ-q and ν_μ-e experiments are perfectly consistent with the global fit, whereas the APV result and the eD asymmetry fit are just 1-σ away. Further studies of polarization asymmetries in the $e - q$ sector, as well as quantitative studies of the neutral current processes at TRISTAN energies might be potentially rewarding.

We can now express the result of our global fit (45) and (42), in terms of the S, T, U parameters and $\bar{\delta}_b(m_Z^2)$. We find

$$\begin{aligned} S &= -0.29 \quad -1.5\,(\alpha_s - 0.12) \quad +0.67\,\delta_\alpha \pm 0.33 \\ T &= \ \ 0.46 \quad -5.7\,(\alpha_s - 0.12) \quad -0.04\,\delta_\alpha \pm 0.37 \\ U &= \ \ 0.39 \quad +5.8\,(\alpha_s - 0.12) \quad +0.24\,\delta_\alpha \pm 0.76 \\ \bar{\delta}_b &= -0.0064 - 0.43\,(\alpha_s - 0.12) \qquad \pm 0.0034 \end{aligned} \qquad \rho_{\rm corr} = \begin{pmatrix} 1 & 0.84 & -0.13 & -0.12 \\ & 1 & -0.29 & -0.31 \\ & & 1 & 0.14 \\ & & & 1 \end{pmatrix} \tag{46a}$$

$$\chi^2_{\rm min} = 5.46 + \left(\frac{\alpha_s - 0.103}{0.0124}\right)^2 + \left(\frac{\delta_\alpha}{0.1}\right)^2 \tag{46b}$$

Only the correlation between the errors in S and T is significant. We show in Fig. 7 the above results. The only radiative effect which is significantly non-vanishing is in the

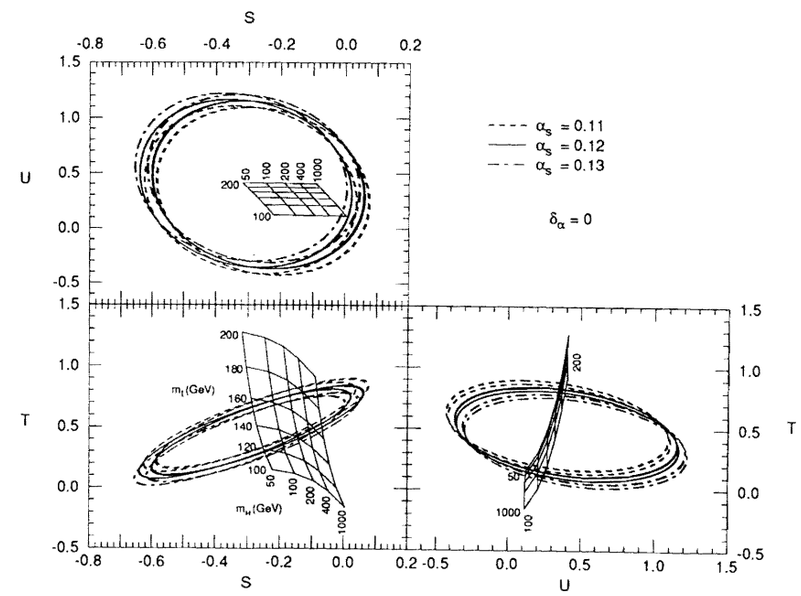

Fig. 7 Global fit to the $(S,\ T,\ U)$ parameters as defined in eq.(11) for three α_s values and for $(m_t,\ m_H)$ values in the range $m_t = 100 - 200$ GeV and $m_H = 100 - 1000$ GeV. Hadronic vacuum polarization contribution to $1/\bar{\alpha}(m_Z^2)$ has been taken to be $(\Delta\frac{1}{\alpha})_{\rm hadron} = -0.0283/\alpha = -3.88$ $(\delta_\alpha = 0)$ [19]. The SM predictions are also given.

T parameter. Both the S and U parameters are consistent with zero at the 1-σ level. Note also that the S parameter is particularly sensitive to the hadronic uncertainty δ_α of $1/\bar{\alpha}(m_Z^2)$, whose mean value can change by a quarter of its error for $\delta_\alpha = \pm 0.10$ [19].

3.4 Testing the Minimal Standard Model

In the minimal SM, the parameters $\bar{g}_Z^2(m_Z^2)$, $\bar{s}^2(m_Z^2)$, $\bar{g}_Z^2(0)$, $\bar{s}^2(0)$, $\bar{g}_W^2(0)$ and $\bar{\delta}_b(m_Z^2)$ are uniquely determined by the two mass parameters m_t and m_H. Insertion of the SM (m_t, m_H) dependences into our global fits (31), (40) and (42) gives the constraints on m_t and m_H.

In Fig. 8, we show the result of our global SM fit to all the electroweak data in the (m_t, m_H) plane for three representative α_s values. One can clearly see the positive correlation between the preferred values of m_t and m_H, which is found independently of the assumed α_s value. On the other hand, the preferred range of m_H depends rather sensitively on α_s. For $\alpha_s(m_Z) \lesssim 0.125$, smaller m_H is preferred, whereas for $\alpha_s(m_Z) \gtrsim 0.130$, larger m_H is slightly favored. The m_H dependence of the fit is very mild and no strict bound on m_H can be given without imposing a constraint on $\alpha_s(m_Z)$.

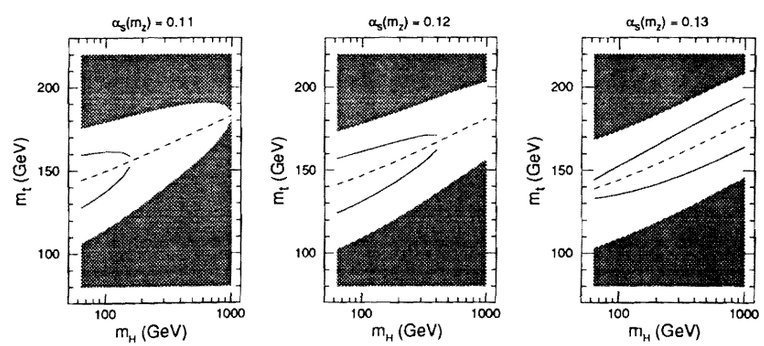

Fig. 8 Electroweak constraints on (m_t, m_H) in the minimal SM, for three selected α_s and at $\delta_\alpha = 0$. Dashed lines show the best m_t values for a given m_H, the solid contors are for $\chi^2 = \chi^2_{\min} + 1$ and the shaded region gives $\chi^2 > \chi^2_{\min} + 4.61$.

We find the following parametrization of our global fit to all the electroweak data in terms of the m_t, m_H, $\alpha_s(m_Z)$ and δ_α:

$$\chi^2_{\rm SM}(m_t, m_H, \alpha_s, \delta_\alpha) = \left(\frac{m_t - \overline{m_t}}{\Delta m_t}\right)^2 + \chi^2_{\min}(m_H, \alpha_s, \delta_\alpha) \tag{47}$$

where

$$\overline{m_t} = 147 + 12.7 \ln\frac{m_H}{100} + 0.9 \ln^2\frac{m_H}{100} - 3\left(\frac{\alpha_s - 0.12}{0.01}\right) - 5\left(\frac{\delta_\alpha}{0.10}\right) \tag{48}$$

$$\Delta m_t = 16 - 0.28 \ln\frac{m_H}{100} - \left(0.044 - 0.006 \ln\frac{m_H}{100}\right)(m_t - 150) \tag{49}$$

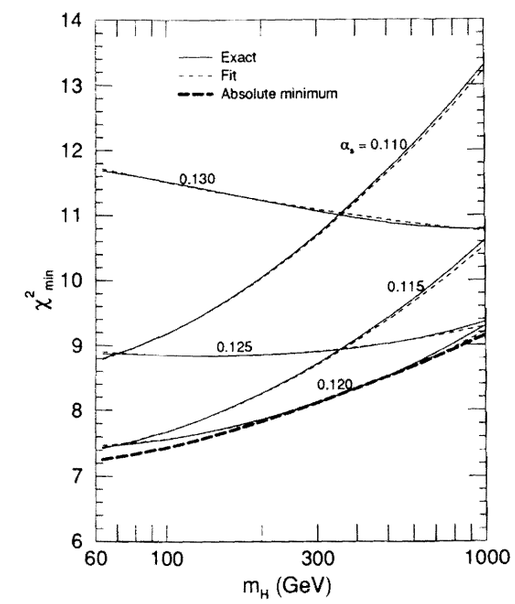

Fig. 9 Minimal of the total χ^2 of the SM fit to all the electroweak data as functions of m_H for $\alpha_s(m_Z)$ =0.110, 0.115, 0.12, 0.125, 0.130. The hadronic vacuum polarization contribution to the effective charge $1/\bar{\alpha}(m_Z^2)$ is obtained by $\delta_\alpha = 0$. The dashed lines show our approximation (50). The absolute minimum which is obtained by allowing both m_t and α_s to be freely fitted by the electroweak data is also shown by a long dashed line.

and

$$\chi^2_{\rm min}(m_H,\alpha_s,\delta_\alpha) = 7.0 + \left(\frac{\delta_\alpha - 0.30}{0.45}\right)^2 + \left(\frac{\alpha_s - 0.1179 + 0.005\delta_\alpha}{0.006}\right)^2 - \left(\frac{\alpha_s}{0.014} + \frac{\delta_\alpha}{0.57} - 8.86\right)\ln\frac{m_H}{100} - \left(\frac{\alpha_s}{0.070} - 1.9\right)\ln^2\frac{m_H}{100} + \left(\frac{\delta_\alpha}{0.10}\right)^2. \tag{50}$$

Here m_t and m_H are measured in GeV units. This parametrization reproduces the correct χ^2 within a few % accuracy in the range $50 < m_t(\text{GeV}) < 300$, $60 < m_H(\text{GeV}) < 1000$ and $0.11 < \alpha_s(m_Z) < 0.13$. The best-fit value of m_t for a given set of m_H, α_s and δ_α is immediately obtained from eq.(48) with its approximate error of (49). Likewise, the dependence of χ^2 on m_H, α_s and δ_α is obtained from the above parametrization for a given set of the remaining parameters. It is also easy to find the results that are independent of α_s or δ_α, or those after imposing external constraints on them, since the χ^2-function above is of a quadratic form in α_s and δ_α which can be readily integrated out. The parametrization also gives accurately the aforementioned α_s dependence of the preferred m_H range, which confirms the trend as observed in refs. [62,63]. As an example, we show in Fig. 9 the minimal of the total χ^2 of the SM fit to all the electroweak data as functions of m_H for selected $\alpha_s(m_Z)$ values. The dashed lines are obtained by using the parametrization (50). Also shown in Fig. 9 is the absolute χ^2 minimum which is obtained by allowing both m_t and α_s to be freely fitted by the electroweak data. Is is approximated as

$$\chi^2_{\rm min} = 7.0 + 0.12[\ln(m_H/14)]^2 \qquad \text{for free } \alpha_s(m_Z). \tag{51}$$

In the region 60 GeV$< m_H < \infty$, this leads to a formal constraint on m_H: $m_H <$ 3.1 TeV (90%$C.L.$). The upper bound is, however, clearly outside the region of validity of our perturbative framework. If we allow an arbitrary m_H values [62], $0 < m_H(\text{GeV}) < \infty$, this bound becomes $m_H < 570\,\text{GeV}$ (90%$C.L.$). Severer upper bound can be obtained by restricting to smaller α_s values ($\alpha_s \lesssim 0.115$), as can be seen from Fig. 9.

Finally, by noting that the effective number of the data we used in our analysis is 18, we conclude, from Fig. 9 and the parametrization (47), that an excellent agreement of the data with the SM predictions is observed in the unshaded ranges of m_t and m_H in Fig. 8 for arbitrary values of α_s and δ_α in the possible ranges; $0.11 \lesssim \alpha_s \lesssim 0.13$ and $-0.1 \lesssim \delta_\alpha \lesssim 0.1$. In other words, we find no signal of new physics beyond the SM in the present precision experiments.

4 Electroweak physics at TRISTAN

In this section, the electroweak physics at TRISTAN is described in our formalism. The charge form factors which would be determined at the TRISTAN energy are $\bar{e}^2(q^2)$, $\bar{g}_Z^2(q^2)$ and $\bar{s}^2(q^2)$ with $\sqrt{q^2} \approx 58$ GeV. It is notable that the measurement of the QED effective coupling $\bar{e}^2(q^2)$ at TRISTAN [64] has a clear advantage over that in LEP/SLC, since the latter receive huge backgrounds from the Z-exchange.

Though most of the formula given in the Z parameter analysis are common for the TRISTAN analysis, it is instructive to repeat them and to express the observables in terms of the scalar amplitudes (4) by neglecting the $\cos\theta$-dependence of the box corrections.

The cross sections for $e^+e^- \to f\bar{f}$ are given by

$$\begin{aligned}\sigma_f &\equiv \sigma(e^+e^- \to f\bar{f}) \\ &= \frac{s}{48\pi}\left\{ \left(\left|M^{ef}_{LL} + M^{ef}_{LR}\right|^2 + \left|M^{ef}_{RR} + M^{ef}_{RL}\right|^2\right)\frac{C_{fV}}{2} \right. \\ &\qquad \left. + \left(\left|M^{ef}_{LL} - M^{ef}_{LR}\right|^2 + \left|M^{ef}_{RR} - M^{ef}_{RL}\right|^2\right)\frac{C_{fA}}{2}\right\}\left(1 + \frac{3}{4}Q_f\frac{\alpha(s)}{\pi}\right),\end{aligned} \tag{52}$$

where the factors C_{fV} and C_{fA} which contains the external QCD corrections for the vector part [29] and for the axial vector part [30] together with the finite mass corrections of the final state fermions [31] are given in eq.(18). Neglecting the lepton masses, we have

$$\sigma_\ell = \frac{q^2}{48\pi}\left\{\left|M^{e\ell}_{LL}\right|^2 + \left|M^{e\ell}_{LR}\right|^2 + \left|M^{e\ell}_{RL}\right|^2 + \left|M^{e\ell}_{RR}\right|^2\right\}\left(1 + \frac{3}{4}\frac{\alpha(q^2)}{\pi}\right). \tag{53}$$

Using the above cross sections, the ratios R_ℓ and R_h at TRISTAN energies are defined by

$$R_\ell = \sigma_\ell/\sigma_{pt}, \tag{54a}$$

$$R_h = \sigma_h/\sigma_{pt}, \tag{54b}$$

with

$$\sigma_{pt} = \frac{4\pi\alpha^2}{3s}. \tag{55}$$

The Forward-Backward asymmetries for $f = \ell, c$ and b are given by

$$A^f_{\rm FB} = \frac{3}{4}\,\frac{2\beta_f\left\{\left|M^{ef}_{LL}\right|^2 + \left|M^{ef}_{RR}\right|^2 - \left|M^{ef}_{LR}\right|^2 - \left|M^{ef}_{RL}\right|^2\right\}}{\frac{3-\beta_f^2}{2}\left\{\left|M^{ef}_{LL} + M^{ef}_{LR}\right|^2 + \left|M^{ef}_{RL} + M^{ef}_{RR}\right|^2\right\} + \beta_f^2\left\{\left|M^{ef}_{LL} - M^{ef}_{LR}\right|^2 + \left|M^{ef}_{RL} - M^{ef}_{RR}\right|^2\right\}}, \tag{56}$$

Table 3 Vertex form factors in the SM at $\sqrt{s} = 58\,\mathrm{GeV}$

f	Γ_1^f	Γ_2^f	Γ_3^f
ν_L	$0.00167 + 0.00198\,i$	$-0.00345 - 0.00261\,i$	—
ℓ_L	$0.00124 + 0.00150\,i$	$-0.00345 - 0.00261\,i$	—
ℓ_R	$0.00013 + 0.00014\,i$	—	—
u_L	$0.00135 + 0.00163\,i$	$-0.00345 - 0.00261\,i$	—
u_R	$0.00006 + 0.00006\,i$	—	—
d_L	$0.00150 + 0.00178\,i$	$-0.00345 - 0.00261\,i$	—
d_R	$0.00001 + 0.00002\,i$	—	—
$b_L\,(m_t = 100)$	$0.00085 + 0.00048\,i$	$-0.00151 + 0.00000\,i$	$-0.00330 + 0.00000\,i$
$b_L\,(m_t = 150)$	$0.00072 + 0.00048\,i$	$-0.00100 + 0.00000\,i$	$-0.00725 + 0.00000\,i$
$b_L\,(m_t = 200)$	$0.00066 + 0.00048\,i$	$-0.00069 + 0.00000\,i$	$-0.01216 + 0.00000\,i$

Table 4 Box form factors in the SM at $s = -2t = (58\ \mathrm{GeV})^2$

f	$sB(e_L, f_\sigma)$	$sB(e_R, f_\sigma)$
ν_L	$0.00051 + 0.00000\,i$	$-0.00003 + 0.00000\,i$
ℓ_L	$-0.00007 + 0.00000\,i$	$-0.00001 + 0.00000\,i$
ℓ_R	$-0.00001 + 0.00000\,i$	$0.00001 + 0.00000\,i$
u_L	$0.00049 + 0.00000\,i$	$-0.00001 + 0.00000\,i$
u_R	$0.00000 + 0.00000\,i$	$0.00000 + 0.00000\,i$
d_L	$-0.00006 + 0.00000\,i$	$-0.00002 + 0.00000\,i$
d_R	$0.00000 + 0.00000\,i$	$0.00000 + 0.00000\,i$
$b_L\,(m_t = 100)$	$-0.00003 + 0.00000\,i$	$-0.00002 + 0.00000\,i$
$b_L\,(m_t = 150)$	$-0.00001 + 0.00000\,i$	$-0.00002 + 0.00000\,i$
$b_L\,(m_t = 200)$	$0.00000 + 0.00000\,i$	$-0.00002 + 0.00000\,i$

with

$$\beta_f = \sqrt{1 - \frac{4m_f^2}{s}}\,. \tag{57}$$

Observable asymmetries for charm and bottom jets should in general have QCD corrections:

$$(A_{\mathrm{FB}}^f)_{\mathrm{obs}} = A_{\mathrm{FB}}^f\Big(1 + k_A\frac{\alpha_s}{\pi}\Big) \tag{58}$$

where the factor k_A depends on details of the jet axis defining algorithm [32].

The magnitudes of the non-universal corrections (vertex and box) in the SM are given in Tables 3 and 4. As seen from Table 4, the box corrections are numerically very small also in this energy region as compared to the propagator and vertex corrections.

We give in Fig.10 the SM predictions for these parameters as functions of $\sqrt{s}$. It should be noted here that the asymmetries are very large because of the large interference between the γ- and the Z-exchange amplitudes. Hence they give qualitatively

different information from the Z-pole asymmetries which determine only the $\bar{s}^2(m_Z^2)$ parameter: the asymmetries at TRISTAN are sensitive to $\bar{g}_Z^2(s)$ as well.

In principle, the TRISTAN experiments as well as those at PEP/PETRA colliders can measure the three charge form factors $\bar{e}^2(s)$, $\bar{g}_Z^2(s)$, $\bar{s}^2(s)$ by assuming the SM

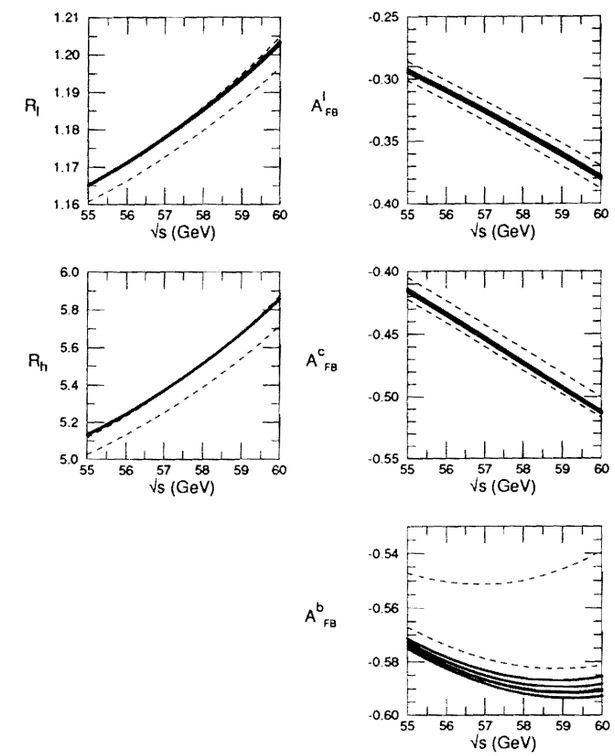

Fig. 10 Obsevables at TRISTAN as functions of $\sqrt{s}$ for $100 < m_t(\mathrm{GeV}) < 200$, $100 < m_H(\mathrm{GeV}) < 1000$ and $\alpha_s = 0.12$. The solid lines show the SM predictions. The regions sandwiched by the dashed lines show the 1-σ allowed predictions that are obtained by using the constraint (59) on the neutral current form factors, and the SM running of all the three form factors with $m_t = 150\,\mathrm{GeV}$ and $m_H = 100\,\mathrm{GeV}$.

dominance to the vertex and box corrections. If we assume the SM running of the $\bar{g}_Z^2(s)$ and $\bar{s}^2(s)$ form factors between the TRISTAN and LEP/SLC energies, then these experiments measure $\bar{e}^2(s)$. On the other hand, if we assume the SM running for $\bar{e}^2(s)$, then they measure two parameters $\bar{g}_Z^2(s)$ and $\bar{s}^2(s)$. This latter measurement has similar physical consequences to those of the low energy neutral current measurements, especially to those of the APV and eD experiments that both measure the neutral currents in the e-q sector. The fits (37) and (39) give the combined information

$$\left.\begin{array}{l} \bar{g}_Z^2(0) = 0.5524 \pm 0.0166 \\ \bar{s}^2(0) = 0.2274 \pm 0.0088 \end{array}\right\} \qquad \rho_{\rm corr} = 0.61, \tag{59}$$

on the neutral current couplings as measured in the e-q sector. The e^+e^- experiments off the Z-peak can give additional information in this sector, as well as the new information in the e-ℓ (purely charged lepton) sector. The SM prediction for these observables are shown by solid lines in Fig. 10. The regions sandwiched by the dashed lines in these figures show the 1-σ allowed predictions that are obtained by using the above constraint (59) on the neutral current form factors, and the SM running of all the three form factors. These regions somewhat deviate from the SM predictions because the present low energy experiments in the e-q sector show 1-σ deviation from the SM predictions with the LEP/SLC inputs: see Figs. 5 and 6. If the e^+e^- experiments find accurate constraints on these observables that are comparable to these predictions of the low energy data, we will effectively have new information on the electroweak physics.

5 Summary

We introduce four charge form factors $\bar{e}^2(q^2)$, $\bar{s}^2(q^2)$, $\bar{g}_Z^2(q^2)$ and $\bar{g}_W^2(q^2)$ associated with the four gauge boson propagators, and one vertex form factor $\bar{\delta}_b(q^2)$ associated with the Zb_Lb_L vertex in the analysis of the electroweak data at the quantum level.

By assuming negligible new physics contributions to vertex and box corrections, except for the Zb_Lb_L vertex, we can determine these charge form factors accurately from precision experiments at the one-loop level. Our approach allows us to test the electroweak theory at several qualitatively different levels. We find that the data show excellent agreement with the SM at all stages of these tests.

We clearly need further improvements in the precision experiments in order to identify a signal of new physics beyond the SM. We find that the two polarization asymmetries at high energies, P_τ and $A_{\rm LR}$, are most effective in this regard since they constrain the parameter $\bar{s}^2(m_Z^2)$ directly without suffering from the QCD uncertainty. At low

energies, two polarization experiments in the e–q sector, the polarized eD scattering and the APV measurements, may have the potential of identifying physics beyond the $SU(2)_L \times U(1)_Y$ universality.

It is also shown that the electroweak physics at TRISTAN can be studied naturally in our framework. It will be an important and exciting work in future to compare and combine the TRISTAN data with the measurements at other energies.

We should note, however, that a better measurement of the QCD coupling strength $\alpha_s(m_Z)_{\overline{\rm MS}}$ and that of the hadronic vacuum polarization effect $\delta_\alpha = \delta[(\Delta\frac{1}{\alpha})_{\rm hadrons}]$ are needed in order for us to look beyond the SM through the electroweak radiative effects.

Acknowledgement

This talk is based on a collaborative work with K. Hagiwara, D.Haidt and C.S. Kim. I would like to thank them for helpful discussions. I would also like to thank N. Ishibashi, Y. Okada, M. Tanabashi, M. Tanaka, I. Watanabe and Y. Yamada for useful comments.

References

[1] J. Ellis, S. Kelley and D.V. Nanopoulos, Phys. Lett. **B260**, 131 (1991);
P. Langacker and M. Luo, Phys. Rev. **D44**, 817 (1991);
U. Amaldi, W. de Boer and H. Fürstenau, Phys. Lett. **B260**, 240 (1991);
G.G. Ross and R.G. Roberts, Nucl. Phys. **B377**, 571 (1992).

[2] J. Hisano, H. Murayama and T. Yanagida, Phys. Rev. Lett. **69**, 1014 (1992).

[3] K. Hagiwara and Y. Yamada, Phys. Rev. Lett. **70**, 709 (1993).

[4] R. Barbieri and L.J. Hall, Phys. Rev. Lett. **68**, 752 (1992.)

[5] K. Hagiwara, F. Halzen and K. Hikasa, Phys. Lett. **141B**, 372 (1984);
H. Murayama and T. Yanagida, Mod. Phys. Lett. **A7**, 147 (1992).

[6] K. Hagiwara, D. Haidt, C.S. Kim and S. Matsumoto, KEK-TH-375 (1993);
K. Hagiwara, S. Matsumoto and C.S. Kim, KEK-TH-375 (1993), plenary talk presented by K. Hagiwara at the *14'th International Workshop on Weak Interactions and Neutrinos* (Seoul, 1993), to be published in the proceedings ; preliminary version of the analysis that introduced the effective charges without pinch terms was reported in K. Hagiwara, *Proceedings of the 10'th International Symposium on High Energy Spin Physics* (Nagoya, 1992), ed. by T. Hasegawa, N. Horikawa and S. Sawada (Universal Academy Press, 1993, Tokyo), p.225.

[7] B.W. Lynn, M.E. Peskin and R.G. Stuart, in *Physics at LEP*, ed. by J. Ellis and R. Peccei, CERN yellow report CERN 86-02 (1986), vol. 1, p. 90.

[8] D.C. Kennedy and B.W. Lynn, Nucl. Phys. **B322**, 1 (1989).

[9] M. Kuroda, G. Moultaka and D. Schildknecht, Nucl. Phys. **B350**, 25 (1990).

[10] M. Consoli, W. Hollik and F. Jegerlehner, in *Z Physics at LEP 1*, edited by G. Altarelli, R. Kleiss, and C. Verzegnassi, CERN 89-08, vol. 1, p. 7.

[11] M. E. Peskin and T. Takeuchi, Phys. Rev. Lett. **65**, 964 (1990); Phys. Rev. **D46**, 381 (1992).

[12] W.J. Marciano and J.L. Rosner, Phys. Rev. Lett. **65**, 2963 (1990);
D.C. Kennedy and P. Langacker, Phys. Rev. Lett. **65**, 2967 (1990); Phys. Rev. **D44**, 1591 (1991);
P. Langacker and M. Luo, Phys. Rev. **D44**, 817 (1991);
R.D. Peccei and S. Peris, Phys. Rev. **D44**, 809 (1991).

[13] G. Altarelli and R. Barbieri, Phys. Lett. **B253**, 161 (1991);
G. Altarelli, R. Barbieri, and S. Jadach, Nucl. Phys. **B369**, 3 (1992).

[14] B. Grinstein and M.B. Wise, Phys. Lett. **B265**, 326 (1991).

[15] K. Hagiwara, S. Ishihara, R. Szalapsky and D. Zeppenfeld, Phys. Rev. **D48**, 2182 (1993).

[16] R. Barbieri, M. Frigeni and F. Caravaglios, Phys. Lett. **B279**, 169 (1992);
G. Altarelli, R. Barbieri, and F. Caravaglios, CERN-TH. 6902/93.

[17] G. Altarelli, R. Barbieri, and F. Caravaglios, CERN-TH. 6770/93.

[18] I. Maksymyk, C.P. Burgess and D. London, McGill-93-13.

[19] H. Burkhardt, F. Jegerlehner, G. Penso and C. Verzegnassi, Z. Phys. **C43**, 497 (1989);
F. Jegerlehner, in *Proceedings of the 1990 Theoretical Advanced Study Institute in Elementary Particle Physics*, ed. by P. Langacker and M. Cvetič ; and private communication.

[20] J.M. Cornwall and J. Papavassiliou, Phys. Rev. **D40**, 3474 (1989);
J. Papavassiliou, Phys. Rev. **D41**, 3179 (1990).

[21] G. Degrassi and A. Sirlin, Nucl. Phys. **B383**, 73 ((1992)); Phys. Rev. **D46**, 3104 (1992);
G. Degrassi, B.A. Kniehl and A. Sirlin, Phys. Rev. **D48**, 3963 (1993).

[22] S. Dawson, J.S. Hagelin and L. Hall, Phys. Rev. **D23**, 2666 (1981).

[23] S. Willenbrock and G. Valencia, Phys. Lett. **B259**, 373 (1991);
R.G. Stuart, Phys. Lett. **B262**, 113 (1991); *ibid.* 353 (1991).

[24] A. Sirlin, Phys. Rev. Lett. **67**, 2127 (1991); Phys. Lett. **B267**, 240 (1991);
A. Leike, T. Riemann and J. Rose, Phys. Lett. **B273**, 513 (1991); see also
D.Y. Bardin, A. Leike, T. Riemann and M. Sachwitz, Phys. Lett. **B206**, 539 (1988).

[25] A. Sirlin, Phys. Rev. **D22**, 971 (1980).

[26] W. Hollik, talk presented at the *XVI International Symposium on Lepton-Photon Interactions* ;
M. Swartz, *ibid* .

[27] The LEP Collaborations, ALEPH, DELPHI, L3, OPAL and The LEP electroweak working group, CERN/PPE/93-157 (August, 1993).

[28] SLD Collaboration, K. Abe *et al.*, Phys. Rev. Lett. **70**, 2515 (1993);
SLD Collaboration, R.D. Elia *et al.*, Mod. Phys. Lett. **A8**, 2237 (1993).

[29] S.G. Gorishnii, A.L. Kataeev and S.A. Larin, Phys. Lett. **B259**, 144 (1991).

[30] Y. Kizukuri, I. Ohba, K. Okano and Y. Yamanaka, Phys. Rev. **D23**, 2095 (1981);
B.A. Kniehl and J.H. Kühn, Phys. Lett. **B224**, 229 (1989); Nucl. Phys. **B329**, 547 (1990);
Y. Kizukuri and H. Ozaki, Phys. Lett. **B258**, 427 (1991);
K.G. Chetyrkin and J.H. Kühn, Phys. Lett. **B308**, 127 (1993).

[31] K.G. Chetyrkin and J.H. Kühn; Phys. Lett. **B248**, 359 (1990);
K.G. Chetyrkin, J.H. Kühn and A. Kwiatkowski, Phys. Lett. **B282**, 221 (1992).

[32] J. Jersak, E. Laermann and P.M. Zerwas, Phys. Rev. **D25**, 1218 (1982);
A. Djouadi, J.H. Kühn and P.M. Zerwas, Z. Phys. **C46**, 411 (1990).

[33] A.A. Akhundov, D.Yu. Bardin and T. Riemann, Nucl. Phys. **B276**, 1 (1988);
W. Beenakker and W. Hollik, Z. Phys. **C40**, 141 (1988);
J. Bernabeu, A. Pich and A. Santamaria, Phys. Lett. **B200**, 569 (1988); Nucl. Phys. **B363**, 326 (1991);
B.W. Lynn and R.G. Stuart, Phys. Lett. **B252**, 676 (1990).

[34] F. Boudjema, A. Djouadi and C. Verzegnassi, Phys. Lett. **B238**, 423 (1990);
A. Blondel, A. Djouadi and C. Verzegnassi, Phys. Lett. **B293**, 253 (1992).

[35] J. Fleischer, O.V. Tarasov, F. Jegerlehner and P.Raczka, Phys. Lett. **B293**, 437 (1992);
G. Bushalla and A. Buras, Nucl. Phys. **B398**, 285 (1993);
G. Degrassi, Nucl. Phys. **B407**, 271 (1993);
K.G. Chetyrkin, A. Kwiatkowski and M. Steinhauser, Mod. Phys. Lett. **A8**, 2785 (1993).

[36] R. Barbieri, M. Beccaria, P. Ciafaloni, G. Curci and A. Viceré, Phys. Lett. **B288**, 95 (1992); CERN-TH. 6713/92.

[37] A. Denner, W. Hollik and B. Lampe, CERN-TH.6874/93.

[38] M. Veltman, Nucl. Phys. **B123**, 89 (1977);
M.B. Einhorn, D.R.T. Jones and M. Veltman, Nucl. Phys. **B191**, 146 (1981).

[39] A. Cohen, H. Georgi and B. Grinstein, Nucl. Phys. **B232**, 61 (1984);
M. Consoli, W. Hollik and F. Jegerlehner, Phys. Lett. **B227**, 167 (1989);
H. Georgi, Nucl. Phys. **B363**, 301 (1991).

[40] J.J. van der Bij and F. Hoogeveen, Nucl. Phys. **B283**, 477 (1987).

[41] J. Fleischer, O.V. Tarasov, F. Jegerlehner, Phys. Lett. **B319**, 249 (1993).

[42] A. Djouadi and C. Verzegnassi, Phys. Lett. **B195**, 265 (1987);
B.A. Kniehl, J.H. Kühn and R.G. Stuart, Phys. Lett. **B214**, 621 (1988);
B.A. Kniehl, Nucl. Phys. **B347**, 86 (1990);
F. Halzen and B.A. Kniehl, Nucl. Phys. **B347**, 86 (1990).

[43] B.A. Kniehl and A. Sirlin, Nucl. Phys. **B371**, 141 (1992); Phys. Rev. **D47**, 883 (1993);
S. Fanchiotti, B.A. Kniehl and A. Sirlin, Phys. Rev. **D48**, 307 (1993).

[44] G.L. Fogli and D. Haidt, Z. Phys. **C40**, 379 (1988).

[45] W.J. Marciano and A. Sirlin, Phys. Rev. **D22**, 2695 (1980).

[46] G. Degrassi, A. Sirlin and W.J. Marciano, Phys. Rev. **D39**, 287 (1989);
A. Góngora-T. and R.G. Stuart, Z. Phys. **C55**, 101 (1992).

[47] A. Sirlin and W.J. Marciano, Nucl. Phys. **B189**, 442 (1981).

[48] CHARM Collaboration, J. Dorenbusch *et al.*, Z. Phys. **C41**, 567 (1989);
L.A. Ahrens *et al.*, Phys. Rev. **D41**, 3297 (1990);
CHARM-II Collaboration, P. Vilain *et al.*, Phys. Lett. **B281**, 159 (1992);
R. Beyer, Dissertation, Univ. of Hamburg, 1991.

[49] S. Sarantakos, A. Sirlin and W.J. Marciano, Nucl. Phys. **B217**, 84 (1983).

[50] S.A. Blundell, W.R. Johnson and J. Sapirstein, Phys. Rev. Lett. **65**, 1411 (1990).

[51] W.J. Marciano and A. Sirlin, Phys. Rev. **D27**, 552 (1983); *ibid.* **D29**, 75 (1984).

[52] C.Y. Prescott *et al.*, Phys. Lett. **84B**, 524 (1979).

[53] J.E. Kim, P. Langacker, M. Levine and H.H. Williams, Rev. Mod. Phys. **53**, 211 (1981).

[54] L. Wolfenstein, Nucl. Phys. **B146**, 477 (1978);
H. Fritzsch, Z. Phys. **C1**, 321 (1979);
T. Oka, Prog. Theor. Phys. **62**, 193 (1979).

[55] J.D. Bjorken, Phys. Rev. **D18**, 3239 (1978);
M. Glück and E. Reya, Phys. Rev. Lett. **47**, 1104 (1981);
S.M. Bilen'kiĭ and G. Motz, Sov. J. Nucl. Phys. **34** 863 (1981).

[56] S. Faifer and R.J. Oakes, Phys. Rev. **D30**, 1585 (1984);
P. Castorina and P.J. Mulders, Phys. Rev. **D31**, 2760 (1985).

[57] J.L. Miramontes, J. Sanchez Guillén and E. Zas, Nucl. Phys. **B264**, 77 (1986).

[58] C.H. Llewellyn Smith, Nucl. Phys. **B228**, 205 (1983).

[59] J.F. Wheater and C.H. Llewellyn Smith, Nucl. Phys. **B208**, 27 (1982); Erratum **B226**, 547 (1983).

[60] CDF Collaboration, talk by D. Saltzberg at the *9'th Topical Workshop on Proton-Antiproton Collider Physics*, Tsukuba, Japan, Oct. 18-22, 1993 ;
D0 Collaboration, talk by Q. Zhu, *ibid.*

[61] A. Denner and T. Sack, Z. Phys. **C46**, 653 (1990).

[62] J. Ellis, G.L. Fogli and E. Lisi, Phys. Lett. **B274**, 456 (1992); *ibid.* **B292**, 427 (1992).

[63] V.A. Novikov, L.B. Okun, M.I. Vysotsky and V.P. Yurov, Phys. Lett. **B308**, 123 (1993).

[64] K. Miyabayashi, talk presented at *the 2nd Workshop on TRISTAN Physics at High Luminosities*, (KEK, Nov.24-26, 1993), to be published in these proceedings.